PUBLIC ROADS

A JOURNAL OF HIGHWAY RESEARCH

UNITED STATES DEPARTMENT OF AGRICULTURE
BUREAU OF PUBLIC ROADS

VOL. 10, NO. 10 ▽ DECEMBER, 1929

FAILURE OF A PORTION OF A RETAINING WALL

For sale by the Superintendent of Documents, Washington, D. C. - - - - - - - - - - - - - - - See page 2 of cover for prices

PUBLIC ROADS

A JOURNAL OF HIGHWAY RESEARCH

UNITED STATES DEPARTMENT OF AGRICULTURE

BUREAU OF PUBLIC ROADS

CERTIFICATE: By direction of the Secretary of Agriculture, the matter contained herein is published as administrative information and is required for the proper transaction of the public business

The reports of research published in this magazine are necessarily qualified by the conditions of the tests from which the data are obtained. Whenever it is deemed possible to do so, generalizations are drawn from the results of the tests; and, unless this is done the conclusions formulated must be considered as specifically pertinent only to the described conditions

VOL. 10, No. 10 **DECEMBER, 1929** **R. E. ROYALL, Editor**

TABLE OF CONTENTS

THE BUREAU OF PUBLIC ROADS
Willard Building, Washington, D. C.

REGIONAL HEADQUARTERS
Mark Sheldon Building, San Francisco, Calif.

DISTRICT OFFICES

DISTRICT No. 1. Oregon, Washington, and Montana.
Box 3900, Portland, Oreg.

DISTRICT No. 2. California, Arizona, and Nevada.
Mark Sheldon Building, San Francisco, Calif.

DISTRICT No. 3. Colorado, New Mexico, and Wyoming.
301 Customhouse Building, Denver, Colo.

DISTRICT No. 4. Minnesota, North Dakota, South Dakota, and Wisconsin.
410 Hamm Building, St. Paul, Minn.

DISTRICT No. 5. Iowa, Kansas, Missouri, and Nebraska.
8th Floor, Saunders-Kennedy Building, Omaha, Nebr.

DISTRICT No. 6. Arkansas, Oklahoma, and Texas.
1912 Fort Worth National Bank Building, Fort Worth, Tex.

DISTRICT No. 7. Illinois, Indiana, Kentucky, and Michigan.
South Chicago Post Office Bldg., Chicago, Ill.

DISTRICT No. 8. Louisiana, Alabama, Georgia, Florida, Mississippi, South Carolina, and Tennessee.
Box J, Montgomery, Ala.

DISTRICT No. 9. Connecticut, Maine, Massachusetts, New Hampshire, New Jersey, New York, Rhode Island, and Vermont.
Federal Building, Troy, N. Y.

DISTRICT No. 10. Delaware, Maryland, North Carolina, Ohio, Pennsylvania, Virginia, and West Virginia.
Willard Building, Washington, D. C.

DISTRICT No. 11. Alaska.
Goldstein Building, Juneau, Alaska.

DISTRICT No. 12. Idaho and Utah.
Fred J. Kiesel Building, Ogden, Utah.

Owing to the necessarily limited edition of this publication it will be impossible to distribute it free to any persons or institutions other than State and county officials actually engaged in planning or constructing public highways, instructors in highway engineering, and periodicals upon an exchange basis. Others desiring to obtain PUBLIC ROADS can do so by sending 10 cents for a single number or $1 per year (foreign subscription $1.50) to the Superintendent of Documents, United States Government Printing Office, Washington, D. C.

THE MECHANICS OF SHEAR FAILURES ON CLAY SLOPES AND THE CREEP OF RETAINING WALLS

By CHARLES TERZAGHI, Research Consultant, United States Bureau of Public Roads

Experience shows that the slides which occur on slopes formed of cohesive earth never take place along planes but along cylindrical surfaces with a very conspicuous curvature. The slides illustrated in Figure 1 may serve as example. The profiles were copied from the classical report of the Swedish Geotechnical Commission on slides which occurred at various places along Swedish railroads (*16*).[1] Figure 2 shows the cross section through a slide which in February, 1918, destroyed 600 feet of a retaining wall at Wembly, along the 4-track main line of the Great Central Railway in England. The maximum depth of the cut was 80 feet and the maximum height of the retaining wall was 30.5 feet with a maximum thickness at the base of 14.5 feet. The underground consisted of "soft clay." From the cross section (fig. 2) it seems probable that the sliding surface passed beneath the base of the wall and intersected the surface at a point beyond the foot of the wall. The clay slides along the slopes of the Hudson River between Albany and Kingston are also distinguished by the strong curvature of the sliding surfaces.

This curvature distinguishes the "shearing slides" from the detritus slides which commonly occur in West Virginia, Ohio, and in southern Pennsylvania (*11*) and which can be described as simple flow phenomena, caused by a temporary decrease of internal friction. Wherever these detritus slides occur in a typical form, they remind one of a skin which starts to peel off the surface of the more stable underground, the thickness of the skin being very small as compared with the length and width. Thus, at the detritus slide of Waeggis in Switzerland, a slide very closely related to those of West Virginia, the width of the moving section of the skin was about 3,000 feet, its length was several hundred feet, and its thickness was not more than about 20 feet. No such proportions are conceivable in connection with a shearing slide, which represents plain rupture rather than a phenomenon of flow.

Hence, whenever investigating the possibility of the occurrence of shearing slides (in contrast to detritus slides or skin movements) along clay slopes, or the stability of retaining walls back filled with clay earth, we are obliged to take the curvature of the sliding surfaces into account; that is, to replace the traditional procedure based on Coulomb's principle (prism of maximum thrust, limited by a plane sliding surface) by other methods.

THEORIES OF CURVED SLIDING SURFACES CAN BE APPLIED FOR SEVERAL PURPOSES

The theories can either be applied to the study of the conditions of equilibrium of sections where slides have already occurred or to the design of the cross section of fills or cuts which have not yet been constructed. In the first case, the coefficients required to make the analysis can be computed from the dimensions of the mass of earth which has moved out, and from the shape of the sliding surface. The procedure in obtaining these data will be described in the following parts of the paper. In the second case, we are obliged to estimate the values of these coefficients either from previous experience with similar materials or from the results of tests performed with the materials in the laboratory.

Sometimes an engineer or a foreman with local experience can tell, with a fair degree of accuracy, the height at which a certain material exposed in a test pit will stand vertically without any support. But their judgment is apt to be unreliable when it comes to estimating the critical height for a slope of 1:1 or 1:2, as shown by a great number of slides which actually have occurred along such slopes. In a case of that kind we can derive the coefficients required for computing the critical height of inclined slopes from the critical height of a vertical slope. A third application is in computing the factor of safety of slopes in places where a slide would be apt to cause severe damages to adjoining properties.

The coefficients required in computing the degree of stability or the factor of safety of slopes are the coefficient of internal friction, tan ϕ (tangent of the angle ϕ of internal friction), and the coefficient of cohesion, c (shearing strength per unit of area, at a surface pressure equal to zero).

FRICTION AND COHESION DISCUSSION

Before engaging in a discussion of friction and cohesion it seems essential to agree on the exact meaning of these terms. Assume that it is desired to determine the resistance to movement of a prism (fig. 3) of earth, JKLM, along some plane, CD, within an embankment. The resistance to movement is a combination of forces due to cohesion and internal friction. The cohesion is due to the attraction existing between the individual soil grains and is independent of the pressure acting upon the surface under consideration. It is a constant value for any unit area within the embankment if the material is uniform.

The internal friction is caused by the resistance to soil grains sliding over each other and varies with the pressure upon the sliding plane. As a result of laboratory experiments the frictional resistance to sliding of an earth prism has been plotted against the load on the sliding plane and found to result in a straight-line relation. The slope of this line (coefficient of internal friction) is the ratio of sliding resistance to pressure upon sliding surface. The angle of which this slope is the tangent is called ϕ, the angle of internal friction.

Let c = cohesion per unit of area of a sliding surface or the coefficient of cohesion,

n = normal unit pressure on sliding surface,

t = shearing resistance (cohesion and friction combined) per unit of area corresponding to a given value of n.

In Figure 3 let n represent the unit pressure normal to the plane CD due to the weight of JKLM.

Then $t = c + n \tan \phi$.

[1] Italic numbers in parentheses refer to bibliography at end of article.

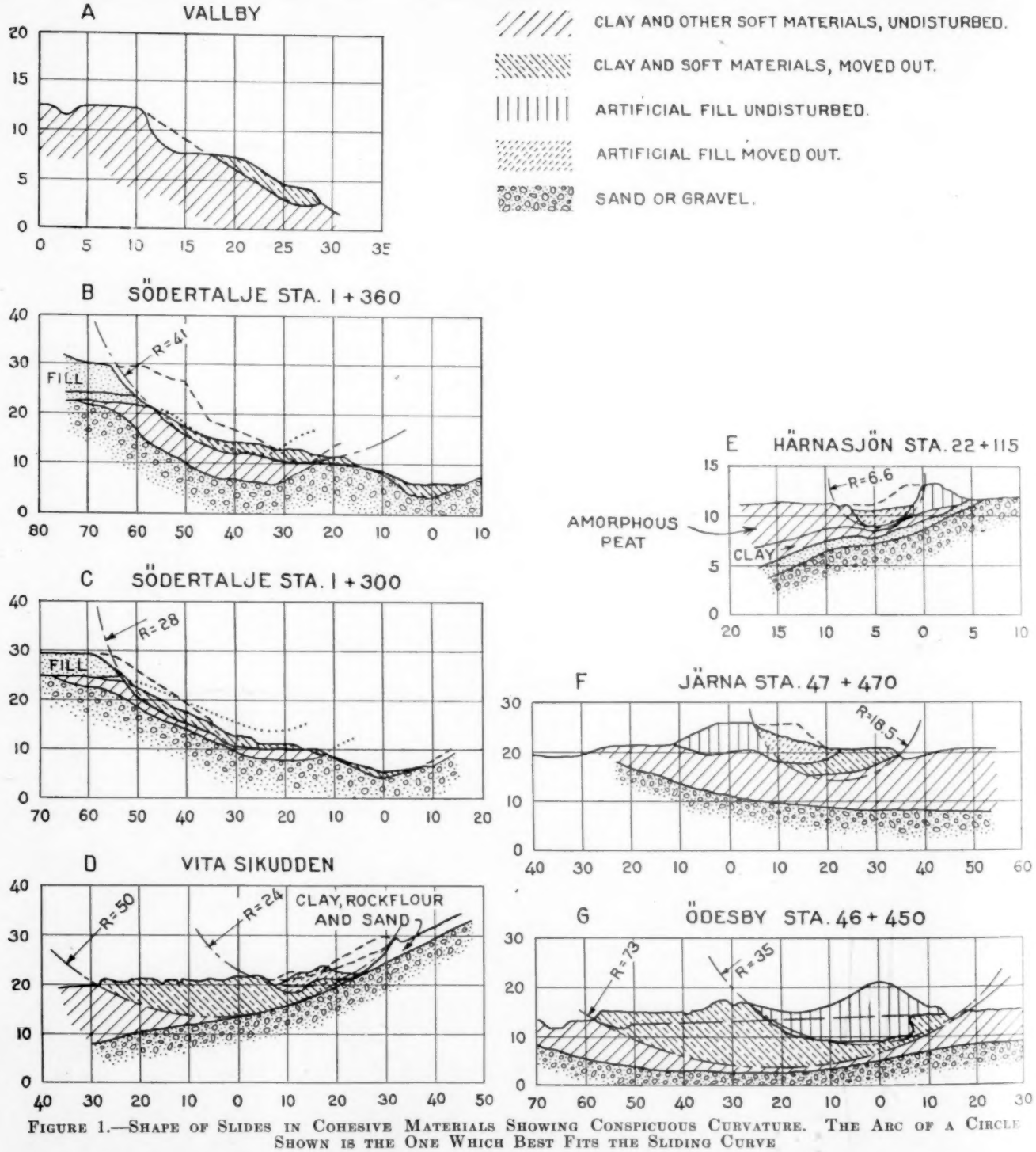

FIGURE 1.—SHAPE OF SLIDES IN COHESIVE MATERIALS SHOWING CONSPICUOUS CURVATURE. THE ARC OF A CIRCLE SHOWN IS THE ONE WHICH BEST FITS THE SLIDING CURVE

The term "critical height" indicates the maximum height of a slope (vertical distance between foot and crest) at which the slope is still stable. Increasing the height beyond this maximum value will cause a slide to occur.

For perfectly cohesionless material (clean dry sand or the like) the angle of internal friction depends to a large extent on the density of the structure. For high densities its value appreciably decreases with the pressure while for low densities the effect of the pressure on the value of the coefficient of internal friction is very small. The tangent of the so-called "angle of repose" is slightly greater than the angle of internal friction for very loose material and slightly smaller than the smallest value of the angle of internal friction of the dense material.[2] Hence the critical height of any slope is equal to infinity, provided the structure of the material is fairly dense and the inclination of the slope is equal to or smaller than the angle of repose.

For practical purposes, one usually assumes the angle of internal friction, ϕ, to be independent of the pressure

[2] These results were obtained from tests recently made at the Massachusetts Institute of Technology under the supervision of the writer and they will be published elsewhere.

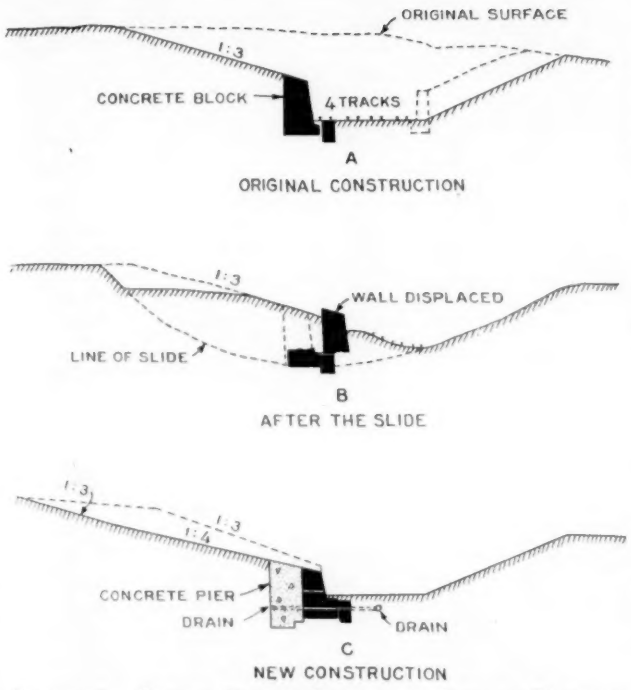

FIGURE 2.—CURVED SLIDING SURFACE OF SLIDE IN RAILWAY CUT IN ENGLAND

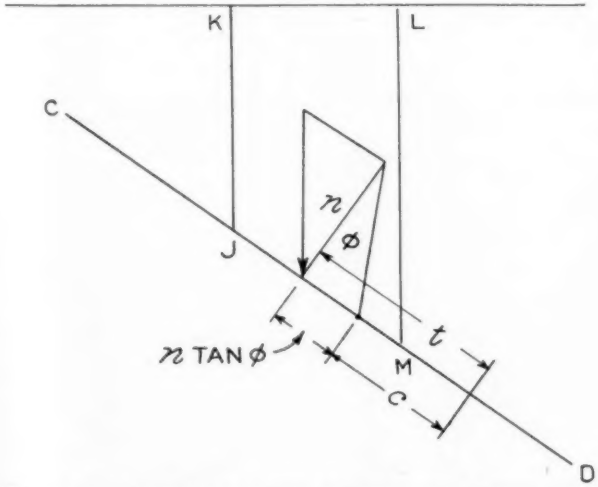

FIGURE 3.—DIAGRAM FOR USE IN EXPLAINING TERMS USED

and equal to the angle of repose. On this assumption, on any plane through a cohesionless material the resistance against lateral displacement is equal to

$$t = n \tan \phi \text{ per unit of area,}$$

where n is the normal pressure perpendicular to the surface. This relation represents the basis of all the earth pressure theories dealing with cohesionless materials. Since the angle of repose can easily be determined, the study of the equilibrium of cohesionless materials does not involve any principal difficulties.

For cohesive materials the resistance, t, against lateral displacement along an interface can be expressed approximately by Coulomb's term

$$t = c + n \tan \phi \quad \text{----------} \quad (1)$$

where c is the cohesion per unit of area. However, in this case the value, ϕ, is very much more difficult to determine than for cohesionless materials, because for materials with even a trace of cohesion, the "angle of repose" has no relation to the angle, ϕ, and may, for the same material, be very different, depending on the height of fill. For a cohesionless material, a given slope is either stable or unstable, regardless of its height.

In contrast to this, for materials with cohesion the maximum angle at which a slope can stand without any support rapidly decreases with increasing height. The value ϕ can be determined only indirectly as from the results of friction tests or by computation from the cross section of slides and from the position of the sliding plane. Many accidents have been caused by assuming the inclination of slopes of cohesive materials as the angle of internal friction.

The difficulties are still greater in defining and determining the value c, because this value depends to a marked degree on the water content of the material. For the same earth, the cohesion increases with decreasing water content. A third complication is caused by the fact that the coefficient of internal friction, tan ϕ, of a cohesive material is very different depending on whether the water content of the earth has or has not an opportunity to adapt itself to changes in pressure. This can easily be demonstrated by the following tests: Suppose we fill two identical containers with identical clay samples and subject the samples to a shearing test under identical pressure. If one of the two samples is placed between sand filters so as to furnish free escape of the excess water while the other sample is sealed off water-tight, the test on the first sample leads to a much higher shearing value than the test on the second one, provided the first sample was tested after the water content had been allowed to adapt itself to the change in pressure.

Many of the leading investigators, among them W. Fellenius (*4*) simply disregard all these existing complications. Such procedure may seem convenient for practical purposes, yet it eliminates the incentive for more profound research and it leaves us in doubt as to the degree of accuracy of our computations. Hence it seems preferable to get, first of all, a conception of the true conditions, and to make the simplifications afterwards with the reservation to modify the procedure as our knowledge increases.

RELATION BETWEEN PRESSURE AND RESISTANCE INVESTIGATED

According to the results of compression tests performed at Massachusetts Institute of Technology on clay specimens subjected to various conditions of internal and external stress, the relation between the pressure, n per unit of area, and the resistance, t per unit of area, against lateral displacement along this area should, for a fat clay, be approximately as shown in Figure 4. When plotting this diagram it was assumed that at the outset the water content of the clay was equal to the liquid limit and, as a consequence, its cohesion practically equal to zero. It was also assumed that the water content could adapt itself to the changes in pressure; that is, with increasing pressure the water content could decrease, and with decreasing pressure the water content could increase.

On gradually raising the pressure from 0 to n_1, the resistance against lateral displacement increases in

direct proportion with the pressure, as it does for a cohesionless material (straight line OP_1); subsequent reduction of the pressure from n_1 to 0 causes the value of t to decrease according to the curve P_1Pc_1, and the effect on t of a following increase of the pressure from 0 to n_2 will be represented by a curve c_1P_2. The two curves P_1Pc_1 and c_1P_2 are far from being identical. They form a hysteresis loop and for the same pressure,

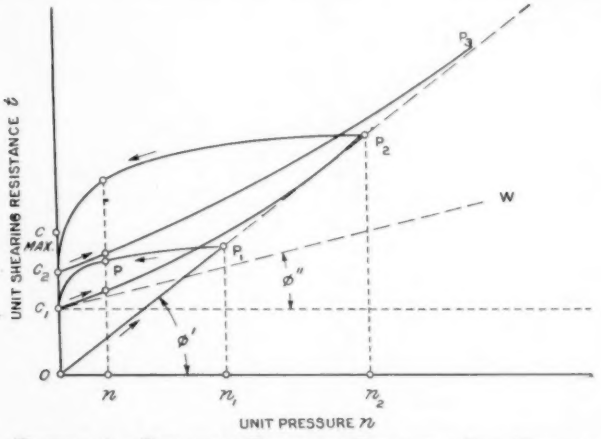

FIGURE 4.—RELATION BETWEEN PRESSURE PER UNIT OF AREA, n, AND RESISTANCE PER UNIT OF AREA AGAINST DISPLACEMENT, t

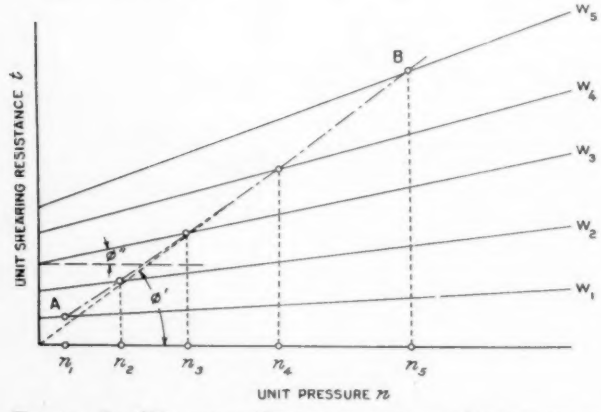

FIGURE 5.—RELATION BETWEEN n AND t ACCORDING TO DR. H. KREY

n, two different values, t, are obtained depending on whether the pressure, n, was approached from the right or from the left. The value of c_1 represents the cohesion produced by the temporary application of the pressure n_1. The greater the pressure, n_1, the greater the value c_1. Yet, even for very high pressures, a certain value of c can not be exceeded ($c_{max.}$) because the value, c, approximately increases with the density of the material, and for very high pressures the increase of density produced by an increase in pressure is very small. If, at the state represented by point c_1 in Figure 4, we prevent the material from giving off any water under the influence of a subsequent increase of the pressure we seem to obtain a straight line c_1W, forming with the horizontal axis an angle ϕ''. The maximum value of c is, for ordinary clays, about 2 kilograms per square centimeter.

Figure 5 represents the relation between n and t according to Dr. H. Krey, of Berlin (*10*). The straight lines W_1 to W_5 determine the resistance against lateral displacement for the water contents w_1, w_2 . . . w_5, provided the water content remains unchanged during the test. On the other hand, if starting with a very soft state and allowing the water content to decrease with increasing pressure, the resistance is said to increase according to the line AB. Although there is some difference between the curves of Figure 4 and Figure 5, which were derived independently by different methods, yet as far as some of the essentials are concerned both conceptions agree and both of them show that formula (1) can be considered only as a radically simplified expression of rather complicated facts.

A considerable part of the uncertainty which still prevails in this field is due to confounding the angles ϕ' and ϕ'' of Figures 4 and 5. As a matter of fact, in most of the papers published on this subject no allusion is made to the wide range through which the angle of internal friction may vary for exactly the same material. To prevent any misunderstanding in this respect, we will define the limiting values ϕ' and ϕ'' as follows:

ϕ' is the angle of internal friction which would be obtained by making a friction test on a very soft sample with insignificant cohesion and proceeding from low toward higher surface pressures, allowing the excess water to drain away before the friction value is measured.

ϕ'' is the angle of internal friction which is obtained by making a friction test on a sample of stiffer consistency and without making provision for the free escape of the excess water.

EXPERIMENTS HAVE RESULTED IN A GENERAL CONCEPTION OF VALUES FOR COHESION AND FRICTION

In practice we usually have to deal with clay deposits which have appreciable cohesion and which, in addition, do not contain any excess water. In order to obtain information on the values ϕ and c for such a material, the friction test should be performed on perfectly undisturbed samples, and provision should be made for the excess water to drain away. The result of such a test would correspond to the curve c_1P_2 or c_2P_3 of Figure 3, and according to the same figure the value of ϕ derived from the test results would not be identical with either ϕ' nor with ϕ''. Because of experimental difficulties no tests have been made up to the present time which have strictly conformed with the requirements indicated here. On the other hand, the considerable number of experiments performed in this field, using widely different methods, result in a general conception of the values for cohesion and friction for the principal types of cohesive earth.

The existing methods for determining these values can be divided into three groups: Measuring the resistance against shear by simple pull (Jacquinot and Frontard, W. Fellenius, A. L. Bell, H. Krey, H. Chatley, Charles Terzaghi, and others); measuring the resistance against shear by rotation (Foundation Committee of the American Society of Civil Engineers, G. Gyldenstein, and others)[3]; and computing the values of the coefficients from the original cross section and from the shape of the sliding surface of earth slides (W. Fellenius, H. Knoke).

[3] Progress report of the special committee to codify present practice on the bearing value of soils for foundations, Proceedings of the American Society of Civil Engineers, vol. 46, No. 6, August, 1920, and vol. 48, No. 3, March, 1922.

In most of the tests included in the first two groups the coefficients were determined while the water content of the material remained practically unchanged, the values of ϕ thus obtained corresponding to the angles ϕ'' of Figures 4 and 5. On the other hand, the tests by the writer were made in such a manner as to give values of ϕ'. Comparing friction values resulting from laboratory tests with values indirectly computed from the shape of sliding curves, it seems that the difference between the values ϕ'' and the values ϕ, on which the stability of clay slopes actually depend, is not very important for fairly stiff clays. Hence in the following sections of this paper the two values ϕ and ϕ'' are considered identical, although it is emphasized that this procedure represents a crude approximation merely warranted by the present lack of a more profound knowledge of the subject. The investigations conducted for the purpose of diminishing the uncertainty concerning the values ϕ and c are still under way, and the results will be published as soon as the tests are terminated.

Table 1 gives a summary of the coefficients c and ϕ determined by various experimenters for different kinds of soils. These data have been used as the basis of an attempt to condense our present knowledge of the values of c and ϕ for the principal types of soils, the result of which is presented in Table 2. More accurate data can not be presented as yet.

THEORIES OF THE EQUILIBRIUM ALONG CYLINDRICAL SLIDING SURFACES PRESENTED

Figure 6 represents a cross section of a slope of a mass of cohesive earth with an angle of inclination, i. If the height of slope, h, exceeds a certain critical value, h_1, a slide occurs as shown in the figure. One of the principal objects of stability computations is the determination of the critical height, h_1, when the values i, c, and ϕ are known. If a theory successfully serves this purpose, it may also be used in connection with any other stability problem concerning cohesive soils. The problem is too complex for accurate solution and the computations must be based on certain simplifying assumptions. One of these assumptions, in common with all the different theories, concerns the validity of equation (1). According to the nature of the other assumptions, we may distinguish between the French method of attack (Résal, Frontard), Becker's attempt, and the Swedish method (Petterson, Sven Hultin, Fellenius, etc.).

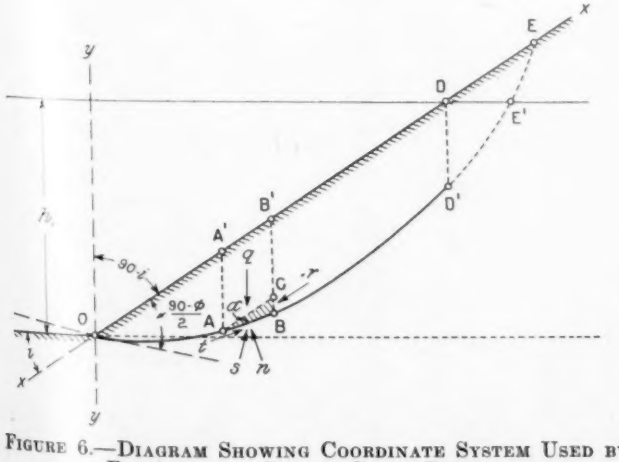

FIGURE 6.—DIAGRAM SHOWING COORDINATE SYSTEM USED BY FRONTARD AND SLIDING CURVE DERIVED

TABLE 1.—*Values of c and φ for cohesive materials*

Experimenter and method	Description of the soil	c in metric tons per sq. m.	φ
CLAYS			
1. Jacquinot and Frontard, sliding test, (*14*).	Loam, very humid	1.93– 2.19	8°
	Loam, fairly dry	2.61– 3.90	8° 40′
	From collapsed earth dam	1.80– 2.68	10° 20′
2. Whangpoo Conservancy District, sliding test (*15*).	Blue, greasy mud	1.12	9° 20′
3. Foundation Com. Am. Soc. of Civ. Eng., rotating device.	Kentucky ball clay, water content 10 per cent.	24.5 –28.0	5° 40′– 7° 30
	Kentucky ball clay, water content 25 per cent.	35.1 –37.8	4° 30′– 5° 40′
	Kentucky ball clay, water content 39.54 per cent.	1.4 – 1.54	0° 16′– 0° 20′
4. A. L. Bell, sliding test (*2*).	Very soft puddle clay	2.14	0°
	Soft puddle clay	3.20	3°
	Moderately firm puddle clay	5.33	5°
	Stiff clay	7.50	7°
	Very stiff bowlder clay	17.20	16°
5. J. H. Griffith, shearing test.	Fairly stiff yellow clay, natural state.	2.14– 3.38	(1)
	Fairly stiff plastic blue clay, natural state.	1.79– 2.53	(1)
6. Chas. Terzaghi, sliding test, provision made for the escape of excess water (*17*).	Pure mud		13°–16°
	Fat blue clay		14°–22°
	Sandy clay		22°–27°
7. W. Fellenius, computed from landslide (*4*).	Soft clay	1.25	4°
8. W. Fellenius, sliding test.	Clay, Järna	.31	4° 30′
9. Gyldenstein, rotating device.	Clay, harbor of Gotenburg, depth of 9 meters, water content 43 to 45 per cent.	.19	9° 30′
10. J. Resal, from general experience with fills (*14*).	Wet soil or hand compacted	1.7	8°
	Almost dry	3.6	
	Very thoroughly compacted	3.6 – 6	
SAND AND GRAVEL			
11. Whangpoo Conservancy Board, China, sliding test (*15*).	Blue mud from Lunghua	2.7	30° 10′
	Sandy mud, Yangtze foreshore.	2.0	30° 10′
	Mud, Pootung point	1.5	28° 00′
12. H. Knoke, computed from existing slopes (*8*).	Cemented gravel	4.7	35°
	Dense sand and gravel mixture.	2.1	35°
	Very dense mixture of sand and gravel.	5.2	40°

[1] Not determined.

TABLE 2.—*Average values of c and φ*

Type of soil	c in metric tons per sq. m.	c in pounds per sq. ft.	φ in degrees
Almost liquid clay	0.5	100	0
Very soft clay	1.0	200	2
Soft clay	2.0	400	4
Medium clay	5.0	1,000	6
Stiff clay	7.5	1,500	8
Muddy sand	2.0	400	30
Very dense sand and gravel	5.0	1,000	34

The French investigators based their theory on the equations which express the conditions for the equilibrium for a very small prismatic element ABC of Figure 6, whose base forms part of the sliding surface OE (*14*). The fundamental assumption was that the stresses, q (produced by the weight of the earth located above AC), and r (lateral pressure) are conjugate stresses. This assumption is also found in Rankine's earth pressure theory, and the results furnished by the theory are as correct or erroneous as this assumption. The stress per unit of area acting on the side AB of the element can be resolved into a tangential stress, t, acting along the surface AB, and a normal stress, n, acting perpendicularly to it. The forces which resist a lateral displacement along AB are,

$$\overline{AB}(c + n \tan \phi) \quad (2)$$

The French investigators determined the position of the element AB by introducing the condition,

$$t - n \tan \phi = \text{maximum} \quad (3)$$

regardless of the absolute value of this maximum. Later in the paper it will be shown that this procedure leads to certain inner contradictions concerning the conditions of equilibrium along the sliding curve. The general equations for the equilibrium of ABC combined with equation (3) lead to

$$-q\cos(\alpha-i)\sin(\alpha-i+\phi)+r\sin\alpha\cos(\alpha+\phi)=c\cos i\cos\phi \quad (4)$$

and,

$$-q\cos(2\alpha-2i+\phi)+r\cos(2\alpha+\phi)=0 \quad (5)$$

These two equations determine for any point, A, of a mass of cohesive earth the angle, ϕ, formed between the slope and the tangent AB to the sliding surface at the point A. Since for every other point of the curved sliding surface, the angle formed between the slope and the tangent to OE should also be equal to α, the differential equation of the curve OE is

$$\frac{dy}{dx}=\tan(i-\alpha) \quad (6)$$

Résal did not succeed in solving this equation, and derived an approximate formula for the critical height, wherein he assumed the critical height to be equal to one-half of the critical height one would obtain if he assumed a plane sliding surface instead of a curved one. His formula is

$$h_1=\frac{c\sin i\cos\phi}{\Delta\sin^2\frac{i-\phi}{2}} \quad (7)$$

wherein Δ is the weight of the earth per unit of volume.

Several years after this formula was published, Frontard (*5*, *6*, *7*) succeeded in solving the differential equation (2). He selected an oblique coordinate system as shown in Figure 6, the two axes forming with each other an angle, $90°-i$, and obtained the following equation for the sliding curve by integration.

$$x=\frac{c\cos\phi\tan i\,(\lambda_0\cos i+\cos\phi\sin\lambda_0-\lambda\cos i-\cos\phi\sin\lambda)}{\Delta\sin(i-\phi)\sqrt{\sin(i-\phi)\sin(i+\phi)}} \quad (8)$$

and

$$y=\frac{c\cos\phi\tan i}{\Delta\sin(i-\phi)\sin(i+\phi)}\left[\frac{\sin\phi}{\tan i}-\sqrt{\sin(i-\phi)\sin(i+\phi)}\sin\lambda+\cos i\cos\lambda\right] \quad (9)$$

wherein λ and λ_0 are auxiliary angles with the values,

$$\tan\frac{\lambda}{2}=\sqrt{\frac{\sin i+\sin\phi}{\sin i-\sin\phi}}\tan\left(\alpha-\frac{i-\phi}{2}\right),$$

$$\tan\frac{\lambda_0}{2}=\sqrt{\frac{\sin i+\sin\phi}{\sin i-\sin\phi}}\tan\left(\frac{\pi}{4}-\frac{i}{2}\right).$$

Frontard demonstrated in addition that the sliding curve OE of Figure 6 consists of two branches with different properties. From O to D′ the sliding surface represented by the curve OD′ is under pressure, while from D′ to E the normal stress consists of tension (value of n negative). Every cohesive soil will crack sooner or later if there is tension, and Frontard concluded the critical height h_1 of the slope is equal to the difference in elevation between O and D. Equations (8) and (9) together with the condition that the normal stress acting on the sliding surface changes at the point D′ from pressure to tension results in the equation:

$$h_1=\frac{2c}{\Delta}\frac{\sin^2 i\cos\phi}{\sin(i-\phi)}\left[\frac{\cos\phi}{\sin i\,(1-\sin\phi)}+\frac{\arccos\frac{\sin^2 i-\sin\phi}{\sin i\,(1-\sin\phi)}}{\sqrt{\sin(i-\phi)\sin(i+\phi)}}\right] \quad (10)$$

The distance DD′ is equal to

$$\frac{2c}{\Delta}\tan\frac{\pi}{4}+\frac{\phi}{2} \quad (11)$$

From a mathematical point of view Frontard's solution is excellent. However, by introducing the fundamental assumption that the stresses, q and r (fig. 6), are conjugate stresses, the problem became overdetermined and there was no possibility of introducing the very essential condition that the forces acting on the wedge ODE are sufficient to overcome the resistance acting along the plane OD′. Without noticing or mentioning this fact Frontard arrived at a curve which fulfills all the essential conditions required for a sliding surface except the one that the forces acting on the earth above the surface are sufficient to produce the movement. The importance of the discrepancy between the acting and the resisting forces is illustrated by a numerical example. Assume a material with the coefficients $c=1{,}950$ kilograms per square meter, $\Delta=1{,}720$ kilograms per cubic meter and $\phi=8°$, corresponding to a fairly soft sandy clay. We wish to determine the critical height for a slope of 2:1 ($\tan i=0.5$, $i=26°\ 34'$).

Résal's formula (7) furnishes the value:

$$h_1=\frac{1{,}950}{1{,}720}\frac{\sin 26°\ 34'\cos 8°}{\sin^2 9°\ 7'}=19.29 \text{ meters}$$

From Frontard's equation (10) we obtain $h_1=8.3$ meters, which is less than half of the value furnished by formula (7). In order to investigate whether the forces acting on Frontard's sliding surface are sufficient to produce a slide, we first used the formulas (8) and (9) for plotting the sliding surface (fig. 7). At O the tangent to the sliding curve forms an angle with the slope of $\frac{90-\phi}{2}=41°$ and for the point D′ the ordinate computed from equation (11) should be identical with the one computed from equation (9). The sliding curve is a deformed cycloid not very different from a circle. Above the point D′ the soil will crack, and, according to Frontard, the maximum height the slope can have without sloughing is equal to the elevation of D above O.

In order to determine if the weight of the body ODE′ is sufficient to overcome both the friction and the

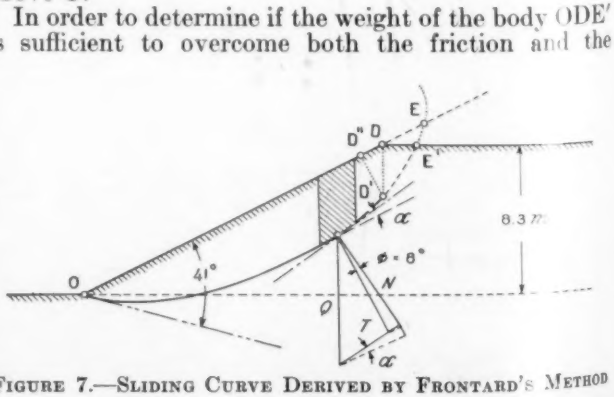

FIGURE 7.—SLIDING CURVE DERIVED BY FRONTARD'S METHOD

cohesion along OE′, the wedge was divided into slices one of which is shown in the figure. The weight of each slice was assumed to be Q. These weights were resolved into tangential components, T, and normal components, N. The force which tends to produce a movement parallel to the slope is equal to $\Sigma T \cos \alpha$. The force which resists the movement is composed of two parts. One of these parts is equal to the sum of all the components of the frictional forces, $N \tan \phi$, or equal to $\Sigma N \tan \phi \cos \alpha = \tan \phi \Sigma N \cos \alpha$. To compute the second part (resistance due to cohesion) we divide the arc OD′ into short sections with a length Δs. Along each one of the sections, Δs, there is a resistance due to cohesion, equal to $c\Delta s$. The component in the direction OD is equal to $c\Delta s \cos \alpha$, and the sum of all these components is $\Sigma c\Delta s \cos \alpha = c\Sigma \Delta s \cos \alpha$. From Figure 7, it is obvious that $\Sigma \Delta s \cos \alpha = \mathrm{OD}''$. Hence the total resisting force is equal to

$$\mathrm{OD}''c + \tan \phi \Sigma N \cos \alpha.$$

The numerical computation disclosed the fact that the driving forces amount to 34.3 tons per meter of width, while the resisting forces are equal to 46.8 tons. Hence, the resisting forces exceed the driving forces by 36 per cent. Due to this inner contradiction caused by the fundamental assumptions, Frontard's solution can be appreciated only as a mathematical achievement. On the other hand, Resal's equation is not backed by sufficiently convincing arguments to make it acceptable for practical purposes.

Another attempt to derive the equation of the sliding curve was made by G. F. Becker in the Report of the Committee of the National Academy of Sciences on the Panama Canal Slides (*1*). However, Becker's theory includes several misinterpretations of the laws of applied mechanics, one of which upsets the validity of the first and fundamental equation of the theory.

Since none of these theories are practical, let us consider the Swedish method, the fundamental principles of which were conceived by K. E. Petterson. This investigator did not attempt to derive the equation of the sliding curve. He assumed that the sliding curve is an arc of a circle, which is in sufficiently satisfactory agreement with what we know from experience, and confined himself to a computation of the resistances (cohesion and friction) required to prevent a movement due to gravity along the cylindrical sliding surface. The method has the obvious disadvantage—that neither the center nor the radius of the arc along which the danger of movement is a maximum can be determined by a direct method of computation unless the conditions of the problem are very simple (uniform slope, homogeneous material). Yet, at present, the method seems to be the only one which gives satisfactory results. Contributions by Sven Hultin, W. Fellenius, and H. Krey, have eliminated the shortcomings of the method to a point where there are no serious obstacles to its practical application.

EFFECT OF INTERNAL FRICTION ON THE POSITION AND THE CURVATURE OF THE MOST DANGEROUS SLIDING SURFACE

The relation which exists between the radius of curvature, the position of the center of the sliding circle, the inclination of the slope, and the coefficient of internal friction was thoroughly investigated by W. Fellenius (*4*). The results published by Fellenius apply only to plane slopes terminating in horizontal planes and consisting of homogeneous material. In solving stability problems with more complicated conditions, the data for finding the position of the dangerous arc must be found by trial. The data furnished by Fellenius makes it possible to select, at the very outset, circles which are fairly close to the critical one and the trial computations can be limited to the investigation of the conditions of equilibrium along a few curves. The

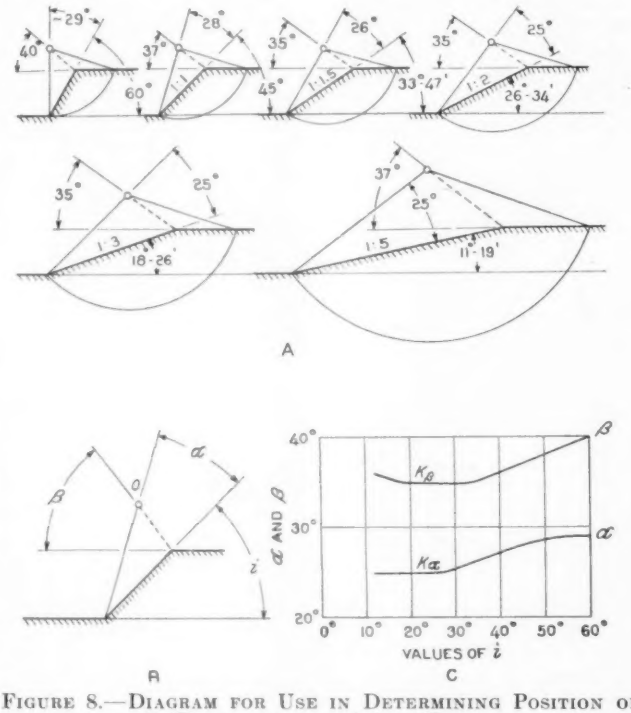

FIGURE 8.—DIAGRAM FOR USE IN DETERMINING POSITION OF O WHEN α, β, AND i ARE KNOWN

following is a brief summary of the data published by Fellenius (*4*):

(*a*) Soils with cohesion only ($\phi = 0$). Figure 8 shows the position of arcs along which the danger of sliding is the greatest, provided the sliding surface passes through the foot of the slope. However, for all slopes with an inclination of less than 53° the most dangerous sliding

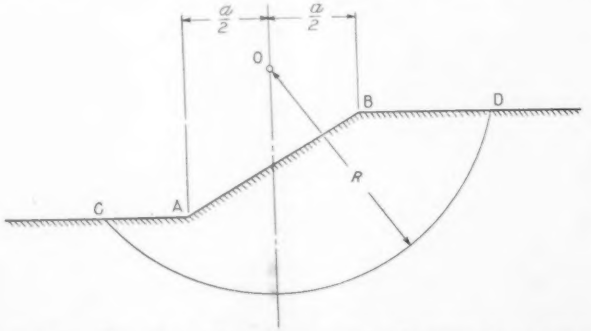

FIGURE 9.—SHAPE OF MOST DANGEROUS SLIDING SURFACE ON SLOPES OF LESS THAN 53°

surface does not pass through the foot of the slope but is located as shown in Figure 9. The center of the critical arc is in this case perpendicularly above the middle of the slope and its radius of curvature should theoretically be equal to ∞. This paradoxical result is due to the assumption, $\phi = 0$. According to Table 1 the angle ϕ is rarely equal to zero and, in addition, the radius of curvature has but very little effect on the

danger of sliding along surfaces located beneath the slope. There is, therefore, no contradiction between theory and practice.

(*b*) Soils with cohesion and friction. For these soils the resistance against sliding at every point of the sliding surface is equal to $c + n \tan \phi$ per unit of surface (equation 1). Since in this case we have to deal with two variables, c and ϕ, the results of a general investigation can only be represented by a set of curves. In order to determine these curves, we start our investigation on the assumption that ϕ is equal to zero. Based on this assumption we determine the cohesion required for maintaining equilibrium. This cohesion value is called c_0, and the centers of the circles along which the sliding would occur are located on a curve

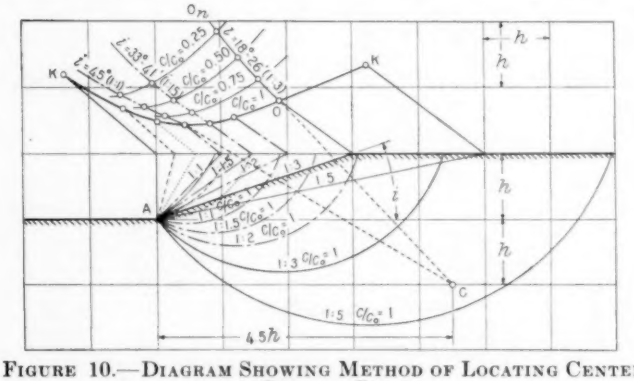

FIGURE 10.—DIAGRAM SHOWING METHOD OF LOCATING CENTER OF SLIDING CURVE

KK. (Fig. 10.) The position of the centers on this curve obviously depends on the inclination of the slope. Now, let us assume that the inclination of the slope remains constant, for instance, $i = 18° 26'$, while the coefficient of friction, tan ϕ, increases. The greater the angle ϕ, the smaller is the cohesion required for maintaining equilibrium. As soon as ϕ becomes equal to the angle of inclination, i, of the slope, the cohesion required for maintaining equilibrium becomes equal to zero. The cohesion values which correspond to the different angles of internal friction will be called c.

The investigations of Fellenius have led to the following conclusions concerning the position of the sliding circles for equal values of i but for different values of ϕ. With increasing values of ϕ the center of the sliding curve (fig. 10) moves from its initial position O ($\phi = 0$, $c = c_0$) up and outward toward O_n, whereby the radius of the sliding circle increases. In the same figure, the dash-dotted curves show the positions of the centers of the sliding circles for different values of ϕ and for values of i of 33° 41′ and 45°. Since the curves on which the centers of the circles are located are very flat, they can, with a sufficient degree of accuracy, be replaced by straight lines. These straight lines approximately pass through a point C, located at a depth of $2h$ below the upper rim of the slope, and at a distance $4.5h$ to the right of the foot of the slope, as shown in Figure 10. Hence, if we determine for any slope the position of the point C and the center O of the sliding circle for $\phi = 0$, we know that the center of the sliding circle for $\phi > 0$ is located on the straight line CO, beyond point O. The position of the center O can be determined by means of the data presented in Figure 8.

In order to investigate the stability of a slope with any arbitrary cross section formed by a material having an angle of internal friction, ϕ, the following procedure is employed.

(1) Simplify the cross section so as to make it conform to one of the standard cross sections shown in Figure 8.

(2) By means of Figure 8, determine the location of the center of the critical circle O, assuming that $\phi = 0$.

Figure 8B shows that the position of O is determined by the value of the angles α, β, and i. If we plot the values of i as abscissas, and the values of α and β as ordinates, we obtain the curves k_α and k_β. (Fig. 7C.) Hence, the position of O for a slope with inclination i may be located by the use of values of α and β corresponding to the value of i as given in Figure 8C.

(3) Determine the position of the point C (fig. 10) and draw the straight line CO.

According to the preceding discussion the point C is located at a depth of $2h$ below the upper level, and at a distance of $4.5h$ to the right of the toe of the slope, h denoting the difference in elevation of the upper and the lower levels of the slope. (See fig. 10.)

(4) On the basis of the data presented in Figure 10 and from previous experience with similar graphic computations, estimate the section of OO_n within which the center of the critical circle for the given value of ϕ will fall.

(5) Within this range select several equally spaced points O′, O″, etc., as centers for the sliding curves.

(6) Draw the sliding curve for each center chosen.

(7) For each curve compute the cohesion, c, required to maintain equilibrium with the assigned value of ϕ. The method of computing c will be explained in the next section of the paper.

(8) The critical sliding plane is obviously represented by the curve for which the value of c is a maximum.

For sliding planes which do not pass through the foot of the slope, an increase of the value of ϕ causes the center of the critical circle to move toward the left and the radius to become smaller, as shown in Figure 11.

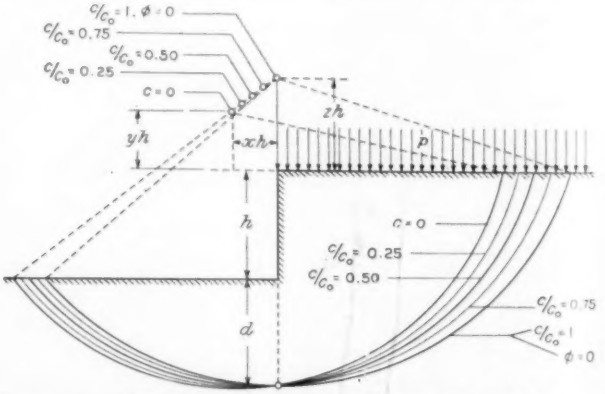

FIGURE 11.—EFFECT OF INCREASE IN VALUE OF ϕ ON LOCATION OF CRITICAL CIRCLE WHERE SLIDING PLANE DOES NOT PASS THROUGH THE FOOT OF THE SLOPE

STABILITY OF COHESIVE EARTH DETERMINED BY SIMPLIFIED GRAPHICAL PROCEDURE

In order to explain the principle of graphically determining the value of c, the cohesion required for maintaining equilibrium along a cylindrical sliding surface, the slice AA′B′B of Figure 6 has been redrawn in Figure 12 on a larger scale. This slice stands under the influence of the following forces; its weight, Q, acting downward, and the two earth pressures E' and E''. These three forces combined give a resultant force R'. Since the slice is supposed to be in equilibrium, the soil located beneath the sliding surface, AB, must exert on the slice a soil reaction equal and opposite to R'. This force is shown in Figure 12 as R. This reaction

can be resolved into a normal force N' and a tangential force T'. (Fig. 12B.) Since the tangential resistance of the soil consists only of cohesion and friction, the condition for the equilibrium of the slice is, $AB\ c + N' \tan \phi = T'$.

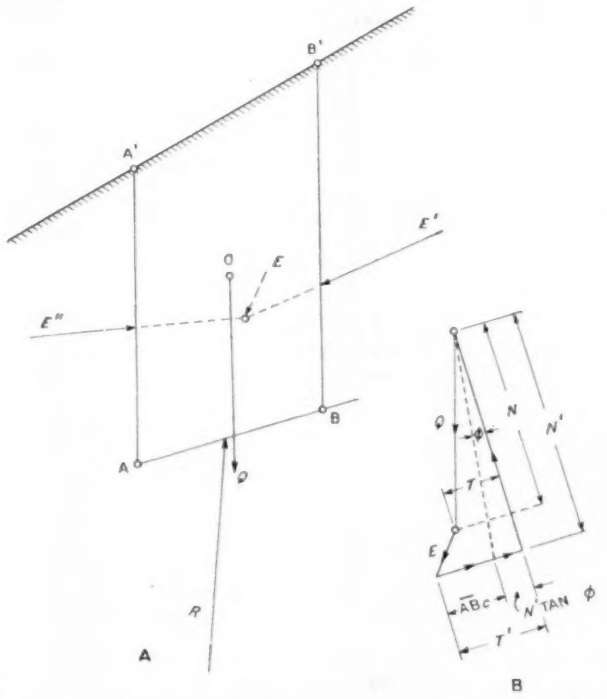

FIGURE 12.—GRAPHIC ANALYSIS OF FORCES ACTING ON SLICE AA'B'B OF FIGURE 6

Unfortunately, neither the direction nor the intensity of the forces E' and E'' are known. In order to solve the problem, it becomes necessary to introduce a more or less arbitrary assumption concerning the forces, E. Sven Hultin assumed that, at each vertical face AA', BB', etc., the forces, E, act at the lower third and in a horizontal direction (*9*). Fellenius assumed the position of the force, E, for the first slice and obtained the data for the other ones from the condition that the polygon of forces for the whole system must be closed (*4*). Whatever the assumption may be, the procedure is rather elaborate and requires a very appreciable amount of time.

However, experience has shown that the effect of the nature of these assumptions has but little influence on the final result of the computation. This is essentially due to the fact that the forces, E, are internal forces of the sliding wedge of earth which in turn leads to both the horizontal and vertical components of the forces, E, balancing each other within the wedge. The sum of all vertical forces acting on the sliding surface is always equal to the weight of the wedge, regardless of what the value and the direction of the E forces may be. Hence, the assumptions concerning E merely influence to a certain extent the distribution of the vertical forces (loads) over the sliding surface.

For these reasons, H. Krey in Berlin suggested disregarding the presence of the earth pressure, E, altogether and making the soil reaction, R (fig. 12A), equal and opposite to the weight, Q, of the corresponding slice. The effect of this simplification on the final result may be learned from the polygon of forces shown in Figure 12B. Taking the forces, E, into consideration, the two components of the soil reaction are T' and N'. Disregarding them, the components are T and N, respectively. In the first case, the resisting forces acting along the surface, AB, are $\overline{AB}c + N' \tan \phi$; in the second case, $\overline{AB}c + N \tan \phi$. The difference is equal to $(N' - N) \tan \phi$. Since for one part of the sliding surface the difference, $(N' - N)$, is positive, for the other one it is negative; the errors partially compensate each other and the final error is generally small enough to be neglected.

To still further reduce the final error, Krey proposed replacing the load system which is represented in Figure 13 by the wedge ABC and the external force, P, by a body of earth, ABD'D, of equal weight but limited by a smooth curve without any corners. This suggestion is based on the fact that every concentrated load spreads over a wider area if transmitted from the surface to a lower level, through an intermediate layer of soil. Thus, in Figure 13, the load, P, will certainly not produce a concentrated pressure acting on the sliding surface, AB, but a more widely distributed pressure of equal intensity. However, Krey points out that, in general, the final error is not important enough to make this procedure necessary.

If one disregards the effect of the forces, E, on the pressure distribution, the stability problem consists merely of determining the sum of the moments $R_1 \Sigma T_n$ which tend to produce a rotation of the wedge around the center of the sliding curve and to determine the sum of the moments which resist such a displacement. Krey solved this problem analytically for a material which has no cohesion ($c = 0$, $\phi > 0$) and tabulated the numerical computations (*9*).

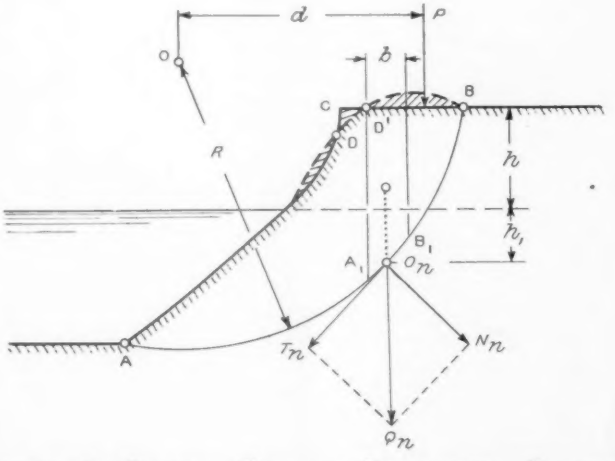

FIGURE 13.—DIAGRAM USED IN DETERMINING COHESION WHERE A SLIDE HAS OCCURRED ALONG CURVE AB

However, based on Krey's simplifying assumption, the whole problem can be handled semi-graphically in a very simple manner, regardless of whether or not the material has cohesion, and whether or not the earth is supported by a retaining wall. The principle of the the procedure is illustrated in Figure 13. To make the case more complicated it was assumed that part of the slope was under water and that a concentrated load, P, per unit of the length of the slope, acted on the upper level near the rim of the slope. Let the weight of the earth above and below the ground water level be equal to Δ and Δ_1 per unit of volume, respectively. Assume

that a slide has occurred along the slope represented in the figure and it is desired to know the cohesion, c, which the material had at the time of the slide, the angle ϕ of internal friction being known.

In order to solve this problem, first determine by means of a survey the position of the sliding surface and pass through the points determined by the survey an arc of a circle, AB. Then draw vertical lines dividing the wedge ABC into slices with a width, b. The weight of each one of these slices is equal to

$$Q_n = b(h\Delta + h_1\Delta_1).$$

The weight, Q_n, of each of these slices can be resolved into a tangential component, T_n, and a radial component, N_n. This operation must be graphically performed for each one of the slices. The sum, ΣQ_n, of the weights of all the slices is equal to the total weight of the wedge ABC. The total cohesion acting along the sliding surface is $\overline{AB}c = Lc$ (where L equals the length of the arc AB) and the total friction is equal to $\Sigma N_n \tan \phi = \tan \phi \Sigma N_n$. Since the movement can consist only of a rotation of the wedge around the center, O, of the sliding surface, the condition for equilibrium is that the sum of all the moments around O must be equal to zero. Hence

$$R\Sigma T_n + Pd = (Lc + \tan \phi \Sigma N_n)\ R, \text{ or}$$

$$c = \frac{T_n + P\frac{d}{R} - \tan \phi \Sigma N_n}{L}$$

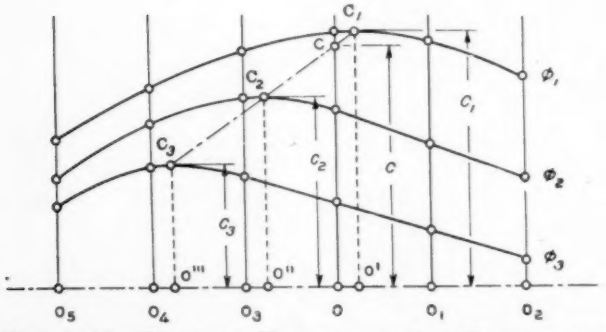

FIGURE 14.—GRAPHICAL DETERMINATION OF COHESION AND ANGLE OF INTERNAL FRICTION

This operation is so simple that it can easily be performed in half an hour. If both the cohesion, c, and the angle of internal friction are unknown, our problems can be presented as follows: Determine the values, c and ϕ, for which the point O represents the center of a most dangerous circle. In order to solve this problem, we assign to the angle of internal friction, ϕ, different values, ϕ_1, ϕ_2, etc., and select several points O_1, O_2, O_3, etc., as centers for different circles which pass through the points A and B. Then we trace these circles and compute for each circle the cohesion required to prevent the slide, provided the angle of internal friction is equal to ϕ_1, ϕ_2, etc. By plotting the distance between the centers of the different circles as abscissas and the values of c, obtained for different values, ϕ_1, ϕ_2, as ordinates, we obtain a set of curves, as shown in Figure 14. Each one of these curves presents somewhere a maximum (C_1, C_2, C_3) whose position determines the position of the center of the most dangerous circle. The slide has obviously occurred along a critical circle. Hence, the intersection C between the dash-dotted curve $C_1C_2C_3$ and the ordinate of O determines the cohesion. From the position of point, C, we learn that the angle of internal friction must have been slightly greater than ϕ_1. This is the general procedure by means of which Fellenius determined the value of ϕ for the underground of the Stigsbergkai in Gotenburg (*4*).

STABILITY DETERMINATION ILLUSTRATED BY A NUMERICAL EXAMPLE

The following numerical example is given to explain the details of semigraphical stability computations:

A uniform slope with an inclination of 1 : 2 (fig. 15) is assumed to consist of a very plastic clay (gumbo) of a medium stiff consistency. The water content was found to be equal to 50 per cent of the weight of the dry substance and the specific gravity of the grains was 2.67. The total height of the slope is 13.5 meters, of which 9 meters are located below the level of an adjoining lake. From previous experience, it is estimated that the angle of internal friction is equal to or somewhat smaller than 4° and the cohesion is approximately equal to 4 metric tons per square meter (about 820 pounds per square foot). Required: To compute the factor of safety of the slope.

Since we are not sure as to the extent to which hydrostatic uplift acts within a mass of plastic clay, the computation will be based on two different assumptions:

I—Hydrostatic uplift fully active, and,

II—Hydrostatic uplift within the clay equal to zero.

The voids ratio of the clay is equal to $0.5 \times 2.67 = 1.335$, and the volume of voids is $\frac{1.335}{1+1.335} = 0.57 = 57$ per cent, the weight of soil above water (provided the voids are completely filled with water) $\Delta = 0.43 \times 2.67 + 0.57 = 1.72$ tons per cubic meter and below the ground water level $\Delta_1 = 0.43 \times 1.67 = 0.72$ tons per cubic meter. The ratio $\frac{\Delta}{\Delta_1}$ is equal to 2.39.

The first step in the investigation is to determine the position of O, the center of the sliding curve, assuming that the angle of internal friction is equal to zero and using the data presented in Figure 8. In this case the slide would occur along the curve AC of Figure 15. Then, the wedge ABC is divided into vertical slices (1), (2), etc., with a width of 4.5 meters each. In order to simplify the graphic procedure for Case I (hydrostatic uplift fully active) multiply the ordinates of the section A_1BC of earth located above the water level by the ratio $\frac{\Delta}{\Delta_1} = 2.4$, which gives the broken line $A_1B_1C_1$. Thus, within the area ABC, the area of every slice of unit depth is proportional to the weight of each slice, for Case II one square meter represents 1.72 tons, and for Case I within the area $AA_1B_1C_1$, every square meter is equivalent to 0.72 ton.

In Case II, the section AA_1 of the slope is acted upon by the water pressure which can be represented by a triangle AA_1W. The side AW of this triangle represents a pressure of 9 metric tons per square meter, which, according to the scale of the drawing is equal to 4.5 centimeters.[4] In order to reduce the water pressures to the scale in which the area ABC represents the weights, connect point $= W_{II}$ with A_1, whereby $AW_{II} = \frac{1}{\Delta} AW = \frac{1}{1.72} \times 4.5$ cm. $= 2.62$ centimeters. W is the resulting force of the water pressures acting on AA_1.

[4] Multiply dimensions of drawing by 1.81 to get dimensions of original drawing.

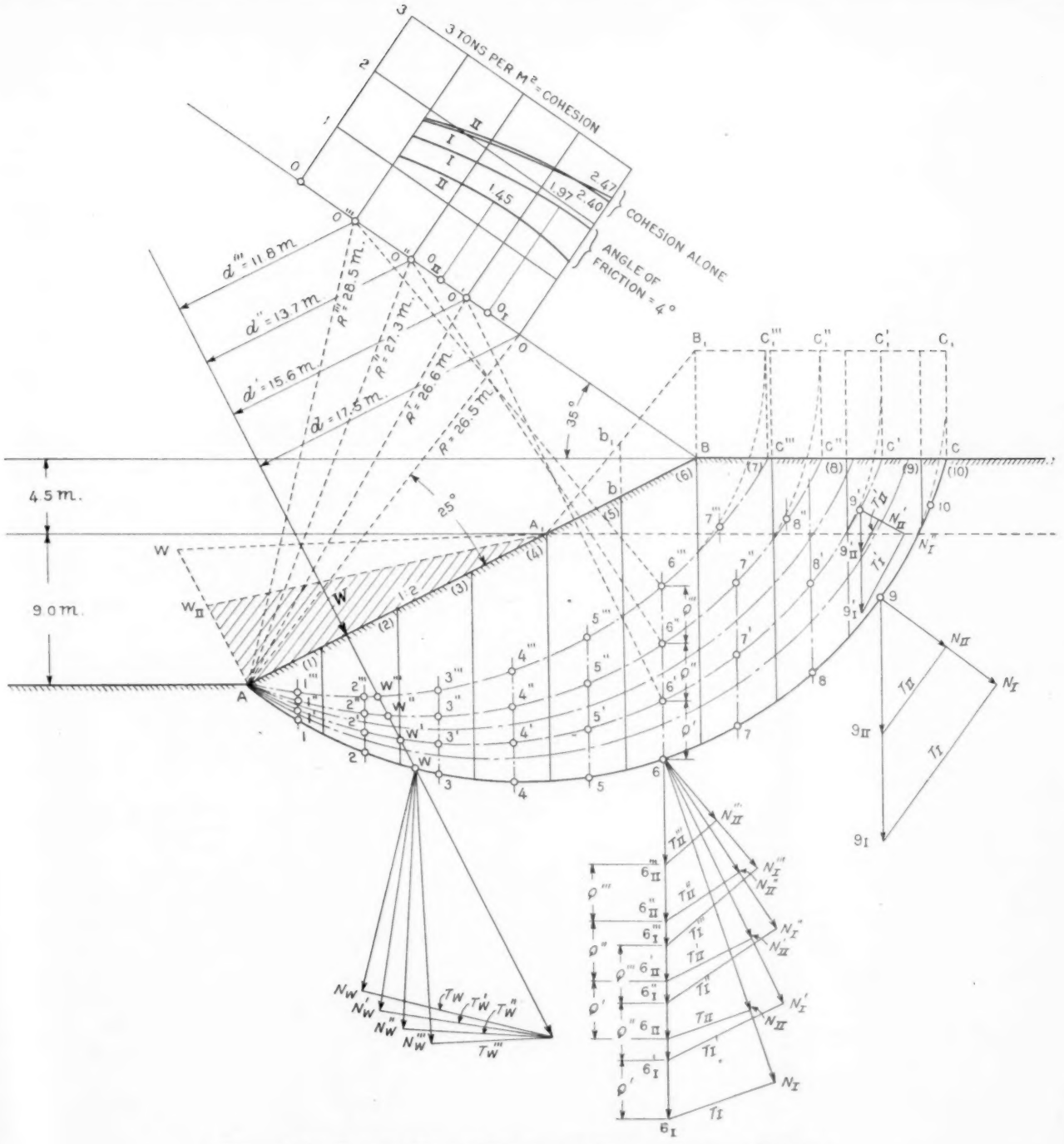

FIGURE 15.—DIAGRAM USED IN SOLUTION OF TYPICAL STABILITY PROBLEM

The following is a summary of the method of performing the investigation:

(1) With the data presented in Figure 8 determine the position of the center O of the circle representing the sliding curve for a plain slope, AB, consisting of earth with cohesion, but no internal friction. In one case the slope, AB, is acted upon by water pressure and in addition the stability of the slope is due not only to cohesion but also to friction. Hence we know in advance that O does not exactly represent the center of the most dangerous circle. But, since we are obliged to determine the position of O by trial, it is already of value to know that it is located in the vicinity of the unknown center and we start our investigation by computing the cohesion required to maintain equilibrium along the arc AC with its center at O.

In order to secure this information, we divide the area ABC into vertical strips, each one of them 4.5 meters wide.

(2) Determine the center of gravity of each one of the slices (1), (2), (3), etc. For most of them the center of gravity can be assumed to be halfway between the two vertical boundaries of the slice.

(3) Pass vertical lines through the centers of gravity of the sections to determine the position of the force of gravity acting on the slices. These forces intersect the sliding curve at the points 1, 2, 3, etc.

(4) Since all the slices are equal in width (except the last one), the weights are proportional to the average heights of the slices. Resolve these weights into radial components, N, and into tangential components, T. In Figure 15 this operation is shown for the point 6 at the base of slice 6. The weight of the slice is represented by the distances $6\text{–}6_I$ and $6\text{–}6_{II}$, respectively (for Case I and Case II, equal to the average height of the slice with the top b_1B_1 and bB respectively). The two components of the weight are N_I, T_I, and N_{II}, T_{II}, respectively.

(5) We proceed in a similar manner for the water pressures represented by the triangle AA_IW_{II}. However, since these water pressures are small in comparison with the total weight of the section ABC, we can replace them by their resultant, W, and resolve this resultant at its point of intersection with the sliding curve W into a radial component N_W and a tangential component T_W.

(6) Assemble the results of these preliminary investigations in a table, indicating the dimensions of the various forces in centimeters as measured on the drawing regardless of the scale. (Table 3.) In Figure 15 all the weights were represented by the average height of the corresponding slices. The width of all the slices was equal to 4.5 meters, except for the slice 10, which was 1.6 meters wide. Hence, in Table 3 all the figures referring to slice 10 were multiplied by the ratio $\frac{1.6}{4.5}$. The measured figures are shown in parentheses with the derived figure below.

TABLE 3.—*Values of N and T for soil slices of Figure 14*

Slice	Case I		Case II	
	N_I	T_I	N_{II}	T_{II}
	Centimeters	*Centimeters*	*Centimeters*	*Centimeters*
1	1.14	−0.70	1.14	−0.70
2	3.40	−1.32	3.40	−1.32
3	5.33	−1.11	5.33	−1.11
4	6.83	−.24	6.83	−.24
5	8.58	+1.18	7.80	+1.07
6	10.33	3.35	8.05	2.60
7	9.90	5.36	7.12	3.83
8	7.47	6.23	5.01	4.17
9	4.30	5.86	2.45	3.32
10	(1.42)	(3.33)	(.50)	(1.14)
	.51	.18	.18	.41
Total	57.79	19.79	47.31	12.03
Total reduced to tons	375	128	733	186

In the original drawing of Figure 15 (before reduction for publication) 1 centimeter represented 2 meters. Hence every centimeter of height of a slice represents 9 cubic meters ($4.5\times2\times1$) of earth. In Case I every cubic meter was supposed to weigh 0.72 tons and in Case II, 1.72 tons. Hence every centimeter scaled off the polygons of forces represents in

Case I, $9\times0.72=6.48$ tons, and in
Case II, $9\times1.72=15.48$ tons.

Multiplying the totals shown in the Table 3 by these factors, we obtain the quantities N_I, T_I, etc., in tons. The components of the water pressure W are $N_W=68$ tons and $T_W=59.5$ tons. Since the sum of the moments of all the forces around the center of rotation, O, should be equal to zero and since, in addition, all the radial forces, N, produce, along the cylindrical sliding surface, a frictional resistance, $N\tan\phi$, in a tangential direction, the conditions for equilibrium are,

for Case I,

$$R\Sigma T_I = R\Sigma N_I \tan\phi + RLc, \text{ or}$$

$$c=\frac{\Sigma T_I-\tan\phi\Sigma N_I}{L}$$

wherein L denotes the length AC of the sliding curve and is equal to 52.3 meters. Hence

$$c=\frac{128-0.07\times375}{52.3}=1.95 \text{ tons per square meter;}$$

for Case II,

$$R\Sigma T_{II}=R\Sigma N_{II}\tan\phi+RLc+RN_W\tan\phi+RT_W, \text{ or}$$

$$c=\frac{\Sigma T_{II}-\tan\phi\Sigma N_{II}-\tan\phi N_W-T_W}{L}$$

$$=\frac{186-0.07(733+68.0)-59.5}{52.3}$$

$$=1.33 \text{ tons per square meter.}$$

In case the angle of friction ϕ were zero, the members which contain $\tan\phi$ would disappear, and we obtain the following:

$$\text{Case I, } c=\frac{\Sigma T_I}{L}=\frac{128}{52.3}=2.45 \text{ tons per square meter,}$$

$$\text{Case II, } c=\frac{\Sigma T_{II}-T_W}{L}=\frac{186-59.5}{52.3}$$

$$=2.42 \text{ tons per square meter.}$$

These figures inform us about the cohesion required to maintain equilibrium along the sliding curve AC.

However, it has been pointed out that the arc, AC, does not represent the most dangerous circle. To find the circle on which the danger of sliding is greatest, we must repeat the computation for several circles. According to the explanation on page 184, the center of the most dangerous sliding surface is located approximately on a straight line connecting B with O. This rule was derived for slopes which are entirely above the water level but it gives at least a hint concerning where to search for the center of the most dangerous circle.

Since shifting the center has little effect on the value of c, for practical purposes it seems to be sufficient to limit the investigation to circles with centers located on a line which passes through B and O. On this line, beyond point O, we select three trial centers O′, O″, and O‴, and draw the corresponding arcs AC′, AC″, and AC‴. The values of c for these arcs can be determined much more rapidly than for the first arc. The procedure is shown for the slice 6. Draw through the point 6 a set of rays, parallel to the lines 6′O′, 6″O″, and 6‴O‴, respectively. In passing from the arc AC to the arcs AC′, AC″, and AC‴ the average height of slice 6 has been reduced in succession by Q', Q'', Q'''. Since in the polygons of forces the weights are represented by the average heights of the slices, to obtain the vertical forces which act within the section 6 on the different sliding planes, it is necessary to reduce the distances $6\text{–}6_I$ and $6\text{–}6_{II}$ in succession by Q', Q'', Q''', thus obtaining the points $6'_I$, $6''_I$, $6'''_I$, and $6'_{II}$, $6''_{II}$, $6'''_{II}$, respectively. Resolve the forces thus obtained into their radial and tangential components N'_I, T'_I, N'_{II}, T'_{II}, etc., and proceed exactly as in the computation for the arc AC.

The results furnished by the computation are plotted above the line OB. Connecting the different points with each other by curves, we determine the position of the centers of those sliding curves, along which the danger of sliding is greatest. The two most dangerous sliding curves ($\phi=4°$, Case I and II) are shown by heavy dash-dotted lines and are located on both sides of the arc AC′. The factor of safety is equal to the ratio between the forces which counteract the movement, and the forces which tend to produce it. Retaining the figures obtained for the sliding curve AC′, and considering that the cohesion of the earth is approximately 4 tons per square meter, we obtain for the factor of safety, S, the following:

$$\text{Case I, } S_I=\frac{\tan\phi\Sigma N+Lc}{\Sigma T}=\frac{0.07\times272+46.4\times4}{110}=1.86$$

$$\text{Case II, } S_{II}=\frac{\tan\phi(\Sigma N+N_w)+\mathrm{L}c}{\Sigma T-T_w}=\frac{0.07(530+73)+46.4\times4}{163.0-53.3}=2.08$$

Considering the hydrostatic uplift to be active is the more conservative assumption. If the internal friction were zero ($\phi=0$), the most dangerous circle would almost coincide with the arc AC, and the factors of safety would be,

$$\text{Case I, } S_I=\frac{Lc}{\Sigma T_I}=\frac{52.3\times4}{128}=1.64$$

$$\text{Case II, } S_{II}=\frac{Lc}{\Sigma T_{II}-T_w}=\frac{52.3\times4}{186.0-59.5}=1.65$$

The assumptions that the sliding surface is strictly cylindrical and that natural soil deposits are perfectly homogeneous give the preceding computations the character of estimates. Hence no great accuracy is required in the numerical computations and the results obtained with an ordinary slide rule are sufficiently accurate.

THEORY APPLICABLE IN DETERMINING THE EARTH PRESSURE AGAINST RETAINING WALLS

The theory of stability of plain slopes may be applied with only slight modification to the earth pressure against retaining walls. For rather steep slopes of clay soil with the lower portion supported by a retaining wall, the curvature of the sliding surface is so appreciable that the theories presented in this paper can be applied in the stability computation. On the other hand, for cohesionless back fills, with either level or gently inclined surface, the curvature of the sliding surface may be neglected and computation may be made using Coulomb's theory, based on the prism of maximum thrust, resting on a plane sliding surface.

In applying any earth pressure theory in the design of retaining walls, two facts should be kept in mind and carefully considered. The first is that the earth pressure theory merely furnishes the lower (or the upper) limit of the earth pressure, known as the active (or passive) earth pressure. If a retaining wall is perfectly rigid and provision is made to prevent it from moving in any direction, the pressure which acts on it may be called "earth pressure at rest." The intensity of this earth pressure lies somewhere between the value of the active and the passive earth pressure. It depends not on cohesion and internal friction, but solely on the elastic properties of the back fill. For this reason it can not be computed by means of earth pressure theory.

However, if the wall is allowed to yield under the influence of the pressure, the intensity of the pressure gradually decreases until finally a shearing surface is formed within the back fill and the "sliding wedge" moves down and outward. The earth pressure which acts against the wall at the instant before the actual shearing occurs is called the "active earth pressure" and represents the smallest value the earth pressure seems to assume. On the other hand, if the wall is prevented from yielding, and, in addition, we press it against the back fill, the intensity of the earth pressure gradually increases, until finally sliding occurs along a slightly curved surface, the sliding wedge moving upward between the wall and the surface of rupture. The earth pressure which acts immediately before this occurs is called the "passive earth pressure." The "earth pressure at rest" differs from the active and the passive earth pressure in that they are independent of the elastic properties of the back fill and merely depend on the cohesion and friction values.

From the preceding discussion it is obvious that the earth pressure does not assume the limiting values before it has undergone a more or less appreciable lateral expansion (or compression) associated with a yield (or advance) of the wall. This fact has been repeatedly demonstrated by experiments and is due to the universal phenomenon that internal friction does not develop before the mass has undergone a certain deformation, comparable with the deformation required to put a solid body under stress. A discussion of the relation which exists between earth pressure and the yielding of the retaining wall may be found in previous publications of the writer (*18*).

SEASONAL VOLUME CHANGES OF BACK FILL OF GREAT IMPORTANCE

From a practical point of view, a second factor—the effect of seasonal volume changes of the back fill on the intensity of the earth pressure—is far more important than the factors just mentioned. These seasonal pressure variations have very little in common with the variation of the pressure exerted by cohesionless materials, due to temperature changes (*3*). In contrast to the temperature effects which are of very little importance, the detrimental pressure variations are only apt to be encountered in those cases where the wall is back filled with clay soils or stone-clay mixtures with appreciable cohesion. Taking the cohesion of these materials into consideration, the earth pressure exerted by the back fill against low retaining walls should, according to the earth pressure theories, be practically zero. Yet these walls are apt to be gradually forced out of plumb in spite of the fact that theoretically they are very often strong enough to stand even the pressure of a cohesionless back fill. This contradiction has led to the conclusion that cohesion is a factor that can not be depended upon, and that the yielding of the walls is due to the cohesion temporarily ceasing to exist.

This conclusion obviously is a fallacy. If cohesion is a factor which can not be depended upon, none of our road and railroad fills, consisting of clay soils, and very few of our earth dams would exist because their slopes are without exception very much steeper than the angles of internal friction presented in Table 2. Cohesion is, within certain limits, as reliable a

factor as is the compressive strength of our construction materials. Hence, if in certain cases cohesive back fills exert earth pressures equal or even in excess of the earth pressures exerted by cohesionless materials of equal weight, the cause must be due to some factor other than those taken into consideration in earth pressure theories.

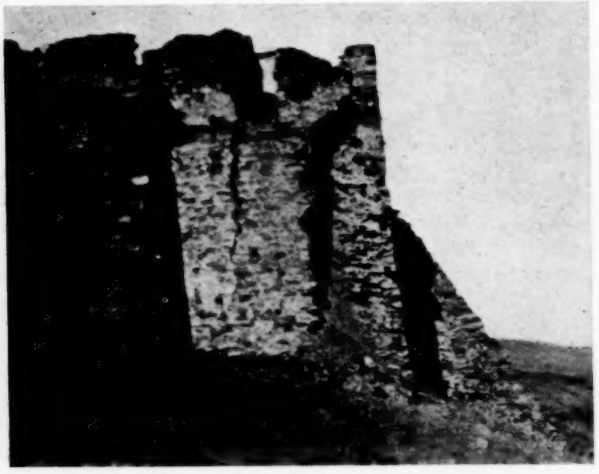

FIGURE 16.—RETAINING WALL ON A HILL WEST OF THE BOSPORUS NORTH OF CONSTANTINOPLE

The explanation of this strange phenomenon can be based on the results of actual observations without the aid of the unwarranted hypothesis that cohesion is not dependable. Figure 16 shows a retaining wall 25 feet high with simple dimensions, reinforced by heavy buttresses. This wall stands on a hill west of the Bosporus and north of Constantinople. During the 25 years of its existence the front part was gradually forced out of plumb, the crest advancing through a distance of about 2½ feet. A piece of the wing wall broke off and became wedged in the upper part of the cleft which separates the wing walls and the front wall. The back fill is a cohesive mixture of stones, grit, sand, and clay, and there is little doubt that the

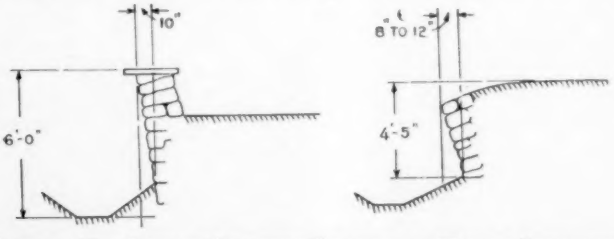

FIGURE 17.—SKETCH SHOWING SHOVING OF TOP OF RETAINING WALL

wall could be removed without causing the back fill to slide.

The retaining wall shown on the cover page (Anadoli Hissar, Asia Minor) is of dry masonry, affording free drainage, and is back filled with a material similar to the back fill of the wall of Figure 16. In the course of some thirty years, some sections of the wall had advanced through a distance of more than 2 feet, and in three places it had collapsed. Figure 17 shows the cross section of two very low retaining walls back filled with cohesive material (loam soil). In this case, due to the very small height of the walls, there can be no doubt that the earth pressure which originally acted on these walls was equal to zero. Yet, in the course of time, they underwent the important deformations shown in the drawing. Figure 18 illustrates the large angle at which a back fill stood immediately after the retaining wall went out.

FIGURE 18.—CONDITION OF BACK FILL AFTER FAILURE OF RETAINING WALL

Near the coast of the Bosporus, between Pera and Bebek, there is a retaining wall with a vertical face, well built and about 60 feet high. In one place the upper half of the wall had bulged, forming a projection about 2 feet beyond the original face of the wall. Investigation disclosed that there was a sewer pipe buried in the back fill which leaked at the spot of the bulging, causing partial saturation of the ground. The bulging developed within about 20 years, because nobody was interested in stopping the leak.

Instructive examples of gradual forward movement of retaining walls may be found on the bridge abutments of several highway bridges in Massachusetts. One of these abutments, located on the Merrimac River, has a height of 23 feet, is of granite masonry faced with cut stone, has a width at the crest of 6 feet 1 inch and at the base of 12 feet, is supported by piles 20 feet long, and is well built. The bridge was constructed 26 years ago in five spans of 207 feet each, with the middle span a draw span. One abutment moved forward gradually and remained approximately parallel to its original position. In order to keep the draw span in working condition the draw tenders were obliged to saw a piece off the wooden plank flooring every summer. At present the abutment is separated from the wing walls by cracks about 3¾ inches wide. Figure 19 shows one crack. The abutment itself shows a vertical crack near the center line of the bridge which seems to indicate that the abutment broke by bending prior to the separation between the wing walls and the abutment.

On a highway bridge in the vicinity of Boston a 20-foot abutment has advanced sufficiently during the last 25 years to put tension members of the bridge truss under compression and cause them to bulge. In a third case the clearance between the parapet and the steel pedestal of the bridge has decreased to zero since the bridge was erected in 1898. There are undoubtedly many cases of this kind, but very little or nothing has been published concerning this important phenomenon, so that the engineering profession has remained practically ignorant of the existence of a very wide gap in our knowledge concerning abutments and retaining walls.

There may also be a causal connection between the gradual advance of retaining walls and the known fact

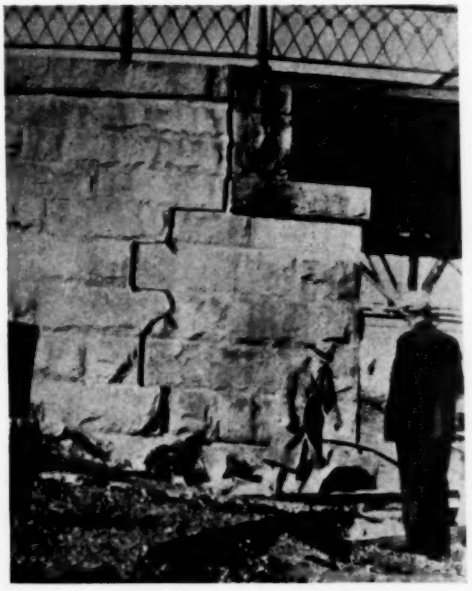

FIGURE 19.—CRACK SEPARATING ABUTMENT FROM WING WALL. HIGHWAY BRIDGE CROSSING MERRIMAC RIVER, MASS.

that the strip of fill next to the retaining wall usually represents a seat of trouble, caused by irregular settlements and other displacements. The writer has observed a concrete gutter located next to the crest of a retaining wall which cracked year after year, in spite of patching and repairing every summer. The cracks were such that they could not be accounted for by the shrinkage of the concrete.

The aforementioned bridge abutments of Massachusetts were amply strong to withstand the earth pressure even with cohesion temporarily absent. Hence, according to the earth pressure theory, they should not move at all. Since the gradual movement can not possibly be accounted for by the earth pressure theory, it is obvious that it is caused by processes other than plain gravity action.

PHENOMENA EXPLAINED BY TEST RESULTS

The phenomena become self-evident when we consider the properties connected with the cohesion of the back fill. These properties are, according to soil physics, low permeability, appreciable volume changes associated with drying and wetting and a very considerable difference between the coefficients of static and hydrodynamic internal friction. Every prolonged dry spell causes the back fill to shrink. Due to gravity action, shrinkage occurs, at least in the deeper parts of the back fill, in a vertical direction only. During the following wet season, the back fill swells slightly and while swelling it exerts not the active but the passive earth pressure which, for a cohesive back fill, may be fifty or more times greater than the active pressure. However, due to the very nature of swelling, the passive pressure ceases to act as soon as the wall has yielded through a distance equal to the lateral expansion of the back fill. During the following dry season the back fill contracts again, without the wall returning to its original position. The following wet season brings an additional lateral yield, and so on.

These seasonal variations of pressure are beyond the field covered by the earth pressure theories because they are caused by factors which are not considered. Their existence is plainly brought out by the pressure

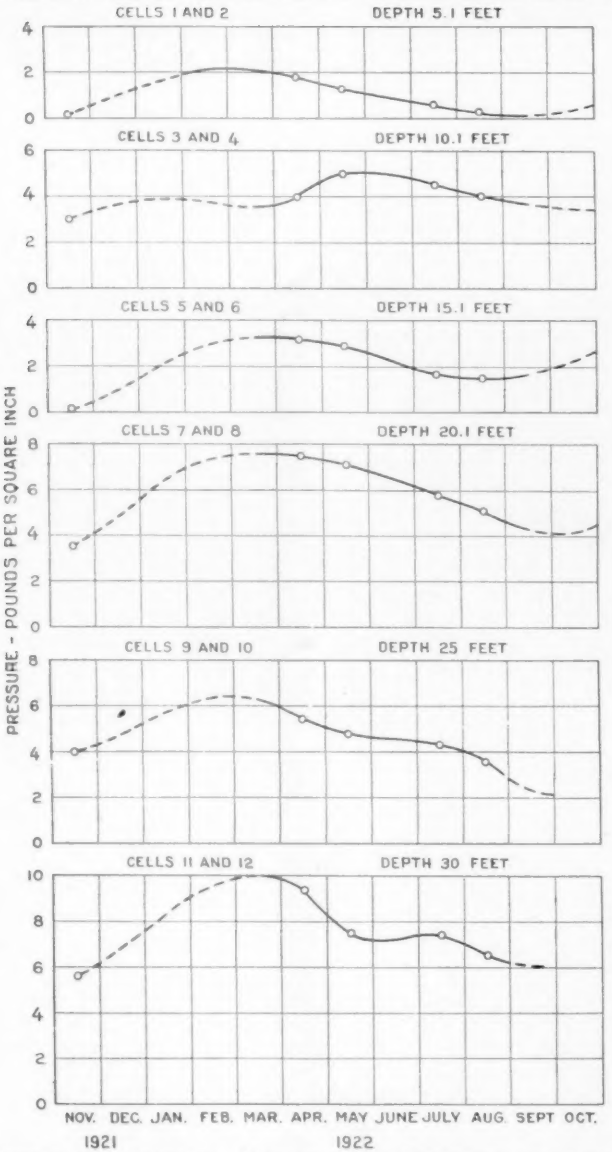

FIGURE 20.—SEASONAL VARIATION IN PRESSURE ON CELLS PLACED BEHIND ABUTMENT OF SKELLIT FORK BRIDGE

cell observations made by the Bureau of Public Roads in 1921–1923 at the abutment of the Skellit Fork Bridge in Illinois (*12*). Plotting the cell pressure against the time, for the various sets of pressure cells, (fig. 20) the seasonal variations are clearly evident. Unfortunately, the paper does not contain any data concerning the character of the fill and the movement of the crest of the wall.

Due to the physical causes of the gradual outward movement of retaining walls, the degree of safety of a wall against pure gravity pressure (active earth pressure according to earth pressure theory) has nothing in common with the factor of safety against gradual lateral displacement. The intensity of the active earth pressure (plain gravity pressure) which acts on a wall immediately after it has been back filled depends entirely on the specific gravity, the internal friction and the cohesion of the back fill. On the other hand, the forces which produce the gradual displacement depend on the elastic properties of the back fill, its structure, fineness, and, to a high degree, on the climatic conditions.

The fundamental difference between the two types of action can best be appreciated by recalling the established fact that, in nature, the top strata of all slopes consisting of cohesive earth move like glaciers, slowly but irresistibly, down the hillsides, unless their inclination is smaller than 4° or 5°, the speed depending on the slope, on the nature of the material, and on the climatic conditions (*13*). Slopes consisting of cohesionless material (detritus slopes in desert regions) also move and flatten out, but in this case the movement is exclusively caused by temperature variations (identical with the cause of the pressure variations observed by J. Feld (*3*), and for equal slopes, the speed of the movement is very much less than for cohesive soils in humid climates. With respect to gravity action, a slope with an inclination of 10°, consisting of cohesive soil and in a humid region, may be so amply stable that no slide may occur even on making a side cut with a vertical face 20 feet high. Yet, the same material, prior to making the side cut, may move at a rate of a quarter of an inch per year.

Several facts disclosed the existence of this movement. One of them is the slight curvature of the lower parts of trees which reach a vertical position only at a certain height above the ground. On making a side cut with a vertical face 20 feet high and building a retaining wall with ample dimensions against the face thus obtained, the factor of safety against gradual displacement would be practically zero, because the chances are the crest of the wall will be forced out of its original position with at least the same speed with which the slope moved prior to the construction of the wall. The intensity of the active earth pressure can be computed by means of the earth pressure theory. It would in this case be equal to zero. On the other hand, practically nothing is known concerning the forces which tend to force the wall gradually out of plumb and concerning the resistance required to prevent the outward movement. The scarce data presented in this paper are just sufficient to give us a qualitative conception of the factors involved and to call our attention to the existence of gradual displacements.

From the little experience we have it seems that the heavier the wall the smaller are the displacements per year. It is not yet known whether it is always economically possible to prevent the gradual yield completely. Until the behavior of abutments and retaining walls under different climatic conditions back filled with different materials is systematically investigated we can not even guess in advance the probable speed of the movement or the forces apt to be exerted by the advancing abutments against the bridge trusses.

Gradual outward movements are occasionally observed on sea walls back filled with fine, cohesionless sand and founded on sand or on piles. These movements are caused by factors not covered in this paper which deals exclusively with cohesive soils.

CONCLUSIONS

A digest of the published data concerning friction and cohesion of clay soils discloses the fact that the angle of internal friction of such soils is exceedingly small as compared with the slopes of our cuts and fills. (Table 2.) Hence, the stability of all our clay fills and clay cuts depends essentially on cohesion. Due to this fundamental fact, the factor of safety of slopes with a given inclination rapidly decreases beyond the critical height at which the soil can stand with a vertical face. Hence, a stable fill of a certain height and consisting of a certain clay soil is no indication of stability in a fill of twice that height, with the same slope and consisting of the same material. In computing the factor of safety of a cut or fill, the curvature of the sliding surface must be taken into account, else the results of the computation may be very misleading. The graphical procedure presented in this paper furnishes the means of making stability computations within a few hours.

The figures furnished by the computation of the stability of retaining walls only inform us about the stability of the walls with regard to the forces produced by the inert weight of the back fill (active earth pressure). There exists the possibility of the occurrence of forces which tend to press the wall gradually out of its original position and which are entirely independent of the active earth pressure. No relation seems to exist between these forces and the active earth pressure of the back fill. The intensity of the active earth pressure depends on the unit weight, the internal friction, and the cohesion of the back fill, while the forces which tend to displace the wall gradually depend on the elastic properties of the back fill, its structure, and on the climatic conditions. The current practice for considering the existence of these nongravitational forces consists in computing the retaining walls as if cohesion were nonexistent. Due to the absence of any causal relation between the active earth pressure and the nongravitational forces, this practice, under favorable conditions, leads to structures with an excessive factor of safety and which are uneconomical. On the other hand, under favorable soil and climatic conditions the walls are apt to gradually yield in spite of the apparent additional safety obtained by neglecting cohesion. In order to reduce the uncertainty associated with the design of retaining walls and abutments, a systematic investigation of existing retaining walls and abutments seems highly desirable.

BIBLIOGRAPHY

(1) Becker, G. F. (Geo. F.).
1916. Mechanics of the Panama Canal slides. U. S. Geological Survey, Professional Paper 98-N. Washington, D. C.

(2) Bell, A. L. (Arthur L.).
1915. The lateral pressure and resistance of clay, and the supporting power of clay foundations. Proceedings of Inst. of C. E. Paper No. 4131, vol. 199. London.

(3) Feld, J.
1923. Lateral earth pressure. Trans. Am. Soc. C. E., vol. 86. pp. 1448-1565.

(4) Fellenius, W.
1927. Erdstatische aufgaben. Berlin.

(5) Frontard.
1922. Cycloides de glissement des terres. Comptes Rendues Hebdomadaires de l'Académie des Sciences, 1922, Paris.

(6) ———
1922. Logoides des glissement des terres. Comptes Rendues Hebdomadaires de l'Académie des Sciences, 1922, Paris.

(7) ———
1922. Loi de la hauteur dangéreuse des talus argileux. Comptes Rendues Hebdomadaires de l'Académie des Sciences, 1922, Paris.

(8) Knoke, H.
1925. Uber zahlenwerte der kohäsion beim erddruck. Die Bautechnik.

(9) Krey, H.
1926. Erddruck, erdwiderstand und tragfähigkeit des baugrundes. Berlin.

(10) ———
1927. Rutschgefährliche und fliessende bodenarten. Die Bautechnik 1927, Heft 35.

(11) Ladd, G. E.
1927. Landslides and their relation to highways. Public Roads, vol. 8, No. 2, April, 1927.

(12) McNary, J. V.
1925. Earth pressure against abutment walls measured with soil pressure cells. Public Roads, vol. 6, No. 5, July, 1925.

(13) Penck, W.
1924. Morphologische analyse. Stuttgart.

(14) Resal, Jean.
1910. Poussée des terres, 2iéme partie. Theorie des terres cohérantes. Paris.

(15) Shanghai harbour investigations.
Report to engineer in chief on the physical properties of the soil in the neighborhood of Shanghai. Shanghai Harbour Investigations, Series 1, No. 7.

(16) Statens järnvagärs geotekniska commission.
1914-1922. Slutbetankande 31. May, 1922.

(17) Terzaghi, Karl.
1925. Erdbaumechanik auf bodenphysikalescher grundlage. Leipzig, Franz Deuticke, 1925.

(18) ———
1920. Old earth pressure theories and new test results. Engineering News-Record, vol. 85, p. 632, September, 1920.

ROAD PUBLICATIONS OF BUREAU OF PUBLIC ROADS

Applicants are urgently requested to ask only for those publications in which they are particularly interested. The Department can not undertake to supply complete sets nor to send free more than one copy of any publication to any one person. The editions of some of the publications are necessarily limited, and when the Department's free supply is exhausted and no funds are available for procuring additional copies, applicants are referred to the Superintendent of Documents, Government Printing Office, this city, who has them for sale at a nominal price, under the law of January 12, 1895. Those publications in this list, the Department supply of which is exhausted, can only be secured by purchase from the Superintendent of Documents, who is not authorized to furnish publications free.

ANNUAL REPORTS

Report of the Chief of the Bureau of Public Roads, 1924.
Report of the Chief of the Bureau of Public Roads, 1925.
Report of the Chief of the Bureau of Public Roads, 1927.
Report of the Chief of the Bureau of Public Roads, 1928.
Report of the Chief of the Bureau of Public Roads, 1929.

DEPARTMENT BULLETINS

No. *136D. Highway Bonds. 20c.
257D. Progress Report of Experiments in Dust Prevention and Road Preservation, 1914.
*314D. Methods for the Examination of Bituminous Road Materials. 10c.
*347D. Methods for the Determination of the Physical Properties of Road-Building Rock. 10c.
*370D. The Results of Physical Tests of Road-Building Rock. 15c.
386D. Public Road Mileage and Revenues in the Middle Atlantic States, 1914.
387D. Public Road Mileage and Revenues in the Southern States, 1914.
388D. Public Road Mileage and Revenues in the New England States, 1914.
390D. Public Road Mileage and Revenues in the United States, 1914. A Summary.
407D. Progress Reports of Experiments in Dust Prevention and Road Preservation, 1915.
463D. Earth, Sand-Clay, and Gravel Roads.
*532D. The Expansion and Contraction of Concrete and Concrete Roads. 10c.
*583D. Reports on Experimental Convict Road Camp, Fulton County, Ga. 25c.
*660D. Highway Cost Keeping. 10c.
*670D. The Results of Physical Tests of Road-Building Rock in 1916 and 1917.
*691D. Typical Specifications for Bituminous Road Materials. 10c.
*724D. Drainage Methods and Foundations for County Roads. 20c.
1216D. Tentative Standard Methods of Sampling and Testing Highway Materials, adopted by the American Association of State Highway Officials and approved by the Secretary of Agriculture for use in connection with Federal-aid road construction.
1259D. Standard Specifications for Steel Highway Bridges, adopted by the American Association of State Highway Officials and approved by the Secretary of Agriculture for use in connection with Federal-aid road work.
1279D. Rural Highway Mileage, Income, and Expenditures 1921 and 1922.
1486D. Highway Bridge Location.

DEPARTMENT CIRCULARS

No. 94C. T. N. T. as a Blasting Explosive.
331C. Standard Specifications for Corrugated Metal Pipe Culverts.

TECHNICAL BULLETIN

No. 55. Highway Bridge Surveys.

MISCELLANEOUS CIRCULARS

No. 62M. Standards Governing Plans, Specifications, Contract Forms, and Estimates for Federal-Aid Highway Projects.
93M. Direct Production Costs of Broken Stone.
*109M. Federal Legislation and Regulations Relating to the Improvement of Federal-Aid Roads and National-Forest Roads and Trails. 10c.

SEPARATE REPRINTS FROM THE YEARBOOK

No. 914Y. Highways and Highway Transportation.
937Y. Miscellaneous Agricultural Statistics.
1036Y. Road Work on Farm Outlets Needs Skill and Right Equipment.

TRANSPORTATION SURVEY REPORTS

Report of a Survey of Transportation on the State Highway System of Connecticut.
Report of a Survey of Transportation on the State Highway System of Ohio.
Report of a Survey of Transportation on the State Highways of Vermont.
Report of a Survey of Transportation on the State Highways of New Hampshire.
Report of a Plan of Highway Improvement in the Regional Area of Cleveland, Ohio.
Report of a Survey of Transportation on the State Highways of Pennsylvania.

REPRINTS FROM THE JOURNAL OF AGRICULTURAL RESEARCH

Vol. 5, No. 17, D– 2. Effect of Controllable Variables upon the Penetration Test for Asphalts and Asphalt Cements.
Vol. 5, No. 19, D– 3. Relation Between Properties of Hardness and Toughness of Road-Building Rock.
Vol. 5, No. 24, D– 6. A New Penetration Needle for Use in Testing Bituminous Materials.
Vol. 6, No. 6, D– 8. Tests of Three Large-Sized Reinforced-Concrete Slabs Under Concentrated Loading.
Vol. 11, No. 10, D–15. Tests of a Large-Sized Reinforced-Concrete Slab Subjected to Eccentric Concentrated Loads.

* Department supply exhausted.

UNITED STATES DEPARTMENT OF AGRICULTURE

BUREAU OF PUBLIC ROADS

CURRENT STATUS OF FEDERAL AID ROAD CONSTRUCTION

AS OF

NOVEMBER 30,1929

STATE	COMPLETED MILEAGE	UNDER CONSTRUCTION					APPROVED FOR CONSTRUCTION					BALANCE OF FEDERAL-AID FUNDS AVAILABLE FOR NEW PROJECTS	STATE
		Estimated total cost	Federal aid allotted	MILEAGE			Estimated total cost	Federal aid allotted	MILEAGE				
				Initial	Stage[1]	Total			Initial	Stage[1]	Total		
Alabama	2,070.4	$ 3,204,853.57	$ 1,585,111.05	119.9	21.0	140.9						$ 1,824,530.50	Alabama
Arizona	815.7	3,136,404.99	2,593,759.22	116.1	99.3	215.4	$ 730,336.86	$ 537,952.41	48.5	14.9	63.4	1,453,087.57	Arizona
Arkansas	1,761.7	3,369,265.93	1,558,639.62	142.2	38.2	180.4	131,587.99	46,503.68	1.2	5.1	6.3	1,483,323.79	Arkansas
California	1,780.3	8,344,426.92	3,845,188.08	223.4	10.4	233.8						10,514.84	California
Colorado	1,158.8	4,411,835.28	2,338,098.14	175.2	46.2	221.4	462,710.67	248,940.29	15.4	.5	15.9	1,088,521.26	Colorado
Connecticut	240.2	960,938.89	341,046.83	8.2		8.2	592,813.75	281,405.81	1.4		1.4	541,678.71	Connecticut
Delaware	227.4	999,799.45	422,059.74	38.5		38.5						22,619.12	Delaware
Florida	467.0	3,281,609.54	1,408,774.29	82.8	5.7	88.5	1,620,611.42	810,305.70	19.2		19.2	689,938.48	Florida
Georgia	2,623.3	2,661,332.54	1,197,775.49	128.0	18.2	146.2						1,985,795.21	Georgia
Idaho	1,154.7	1,223,247.75	735,353.84	79.0	10.2	89.2	285,139.80	168,985.44	32.0	14.1	46.1	428,465.44	Idaho
Illinois	2,016.8	15,726,759.69	6,966,369.36	454.2		454.2	528,000.00	264,000.00	18.3		18.3	2,543,083.24	Illinois
Indiana	1,338.0	7,932,298.00	3,734,638.21	239.2		239.2	359,700.00	179,850.00	12.0		12.0	21,891.93	Indiana
Iowa	3,086.8	2,033,737.74	884,839.42	15.1	63.3	78.4						18,307.71	Iowa
Kansas	2,641.2	5,987,424.85	2,485,936.75	341.1	24.4	365.5	841,218.33	408,362.89	32.9	2.8	35.7	13,394.85	Kansas
Kentucky	1,382.1	4,325,694.31	2,056,407.69	247.2	24.3	271.5	46,327.43	23,153.71		6.1	6.1	399,152.72	Kentucky
Louisiana	1,350.4	3,251,628.73	1,625,814.30	140.6		140.6	225,079.24	101,900.86	.1	4.8	4.9	1,066,019.00	Louisiana
Maine	503.1	2,280,963.22	844,526.26	54.2	1.9	56.1	119,547.29	53,871.00	6.2		6.2	959,686.98	Maine
Maryland	624.3	1,438,907.50	669,938.85	54.7	3.0	57.7	233,972.40	27,773.64	6.7		6.7	172,41	Maryland
Massachusetts	629.7	3,079,412.62	917,370.99	40.6	2.8	43.4						1,470,152.10	Massachusetts
Michigan	1,586.5	9,156 046.00	3,989,923.24	221.9	10.4	232.2	1,550,000.00	843,263.31	36.9	12.4	49.3	83,191.99	Michigan
Minnesota	3,992.4	5,370,528.02	1,688,500.00	214.3	102.2	316.5	4,171,207.29	16,000.00	43.1	116.8	159.9	107,000.00	Minnesota
Mississippi	1,746.1	3,131,868.59	1,312,917.93	121.1	17.4	138.5						1,333,444.49	Mississippi
Missouri	2,331.5	8,461,031.63	3,135,576.97	118.2	116.2	234.4	154,441.12	51,895.79	2.5		2.5	182,507.80	Missouri
Montana	1,659.8	7,429,034.76	4,518,392.21	508.9	27.2	536.1	919,057.18	498,663.22	80.3	23.8	104.1	1,942,147.00	Montana
Nebraska	3,584.4	6,596,999.52	3,161,259.34	318.9	173.0	491.9	522,045.45	233,083.77	21.3	17.4	38.7	811,707.25	Nebraska
Nevada	1,139.7	1,060,522.09	942,307.24	100.8	100.8	201.6						51,250.63	Nevada
New Hampshire	350.6	311,808.70	71,580.00	2.7	2.1	4.8	103,115.32	39,915.00	2.7		2.7	83,528.36	New Hampshire
New Jersey	489.6	3,733,703.37	798,560.00	53.1		53.1	1,396,389.48	214,230.00	14.3		14.3	154,890.08	New Jersey
New Mexico	1,912.1	2,560,791.24	1,621,835.14	130.4	.7	131.1	579,469.98	362,560.81	49.4	2.0	51.4	428,071.56	New Mexico
New York	2,372.0	21,958,117.76	4,620,980.55	309.3		309.3	5,497,000.00	852,900.00	56.9		56.9	3,232,815.99	New York
North Carolina	1,748.2	1,251,824.47	625,073.72	75.2	17.1	92.3	231,991.42	115,842.63	19.5	1.1	20.6	1,296,891.54	North Carolina
North Dakota	4,144.9	1,419,660.67	578,307.52	255.0	88.8	343.8	1,363,582.41	700,271.92	261.7	120.5	372.2	54,589.22	North Dakota
Ohio	2,142.2	12,543,917.06	3,891,840.96	225.3	14.0	239.3	5,080,407.57	1,317,441.87	52.7	25.5	78.2	637,313.97	Ohio
Oklahoma	1,629.4	3,145,088.90	1,438,126.52	99.2	24.3	123.5	1,180,686.08	525,929.03	32.1	31.8	63.9	41,798.93	Oklahoma
Oregon	1,152.4	2,458,229.40	1,427,222.43	139.5	43.7	183.2	798,849.97	477,388.99	47.8	19.4	67.2	362,815.05	Oregon
Pennsylvania	2,228.1	14,525,189.89	3,550,626.56	221.3	14.1	235.4	1,192,419.63	298,807.84	19.3		19.3	39,601.35	Pennsylvania
Rhode Island	179.6	1,136,373.68	291,828.70	13.6		13.6						475,876.33	Rhode Island
South Carolina	1,877.3	2,891,110.11	1,059,446.51	104.2	24.1	128.3						329,756.67	South Carolina
South Dakota	3,474.9	3,424,065.67	1,823,897.32	389.6	78.0	467.6	189,779.58	104,378.74	27.9	30.2	58.1	39,192.68	South Dakota
Tennessee	1,234.1	2,095,052.99	928,743.01	72.8		72.8						910,574.21	Tennessee
Texas	6,310.3	17,485,416.69	7,343,876.24	583.7	237.9	821.6	669,541.29	327,883.03	2.9	25.1	28.0	296,619.67	Texas
Utah	944.0	1,686,417.92	1,212,587.58	70.8		70.8	25,012.23	16,245.08				197,950.58	Utah
Vermont	248.5	958,305.33	349,244.96	18.7		18.7						62,872.48	Vermont
Virginia	1,395.0	2,185,783.32	1,031,610.67	109.5	12.3	121.8	698,447.91	310,505.27	18.6	.1	18.7	20,330.88	Virginia
Washington	861.1	5,522,156.24	2,026,600.00	128.4	29.8	158.2	132,407.92	69,000.00	.2	10.4	10.6	210,980.87	Washington
West Virginia	702.5	3,148,938.18	1,277,680.44	70.1	17.1	87.2	142,187.17	71,093.58	6.3		6.3	9,119.69	West Virginia
Wisconsin	2,146.7	8,136,798.10	3,488,735.72	272.1	19.2	291.3						25,976.12	Wisconsin
Wyoming	1,733.4	1,541,928.49	996,132.99	150.0	17.2	167.2	41,252.20	27,082.06		9.6	9.6	12,314.17	Wyoming
Hawaii	39.5	402,261.10	137,426.82	6.6		6.6	562,688.38	247,259.61	16.6		16.6	1,072,664.16	Hawaii
TOTALS	81,441.7	233,559,352.21	95,530,367.52	7,805.3	1,556.5	9,361.8	33,368,004.47	10,674,656.98	996.9	494.4	1,491.3	30,508,107.68	TOTALS

[1]The term stage construction refers to additional work done on projects previously improved with Federal aid. In general, such additional work consists of the construction of a surface of higher type than was provided in the initial improvement.

U. S. GOVERNMENT PRINTING OFFICE: 1929